# Blind Equalization for Tomlinson-Harashima Precoded Systems

Rubyet Adnan

A thesis submitted in partial fulfilment
of the requirements for the degree of
Master of Engineering
in
Electrical and Electronic Engineering
at the
University of Canterbury,
Christchurch, New Zealand.

February 2007

# ABSTRACT

At a communications receiver the observed signal is a corrupted version of the transmitted signal. This distortion in the received signal is due to the physical characteristics of the channel, including multipath propagation, the non-idealities of copper wires and impulse noise. Equalization is a process to combat these distortions in order to recover the original transmitted signal. Roughly stated, the equalizer tries to implement the inverse transfer function of the channel while taking into account the channel noise. The equalizer parameters can be tuned to this inverse transfer function using an adaptive algorithm. In many cases, the algorithm uses a training sequence to drive the equalizer parameters to the optimum solution. But, for time-varying channels or multiuser channels the use of a training sequence is inefficient in terms of bandwidth, as bandwidth is wasted due to the periodic re-transmission of the training sequence. A blind equalization algorithm is a practical method to eliminate this training sequence.

An equalizer adapted using a blind algorithm is a key component of a bandwidth efficient receiver for broadcast and point-to-multipoint communications. The initial convergence performance of a blind adaptive equalizer depends on the higher-order statistics of the transmitted signal. In modern digital systems, Tomlinson-Harashima precoding (THP) is often used for signal shaping and to mitigate the error propagation problem of a decision feedback equalizer (DFE). The concept of THP comes from pre-equalization. In fact, it is a nonlinear form of pre-equalization, which bounds the higher-order statistics of the transmitted signal. But, THP and blind equalization are often viewed as incompatible equalization techniques.

In this research, we give multiple scenarios where blind equalization of a THP-encoded signal might arise. With this motivation we set out to answer the question, can a blind equalizer successfully acquire a THP-encoded signal? We investigate the

combination of a Tomlinson-Harashima precoder on the transmitter side and a blind equalizer on the receiver side. By bounding the kurtosis of the THP-encoded signal, we show that THP actually aids the initial convergence of blind equalization. We find that, as the symbol constellation size increases, the THP-encoded signal kurtosis approaches that of a uniform distribution, not a Gaussian.

We investigate the compatibility of blind equalization with THP-encoded signals for both SISO and MIMO systems. In a SISO system, conventional blind algorithms can be used to counter the distortions introduced in the received signal. However, in a MIMO system with multiple users, the other users act as interferers on the desired user's signal. Hence, modified blind algorithms need to be applied to mitigate these interferers. For both SISO and MIMO systems, we show that the THP encoder ensures that the signal distribution approaches a non-Gaussian distribution. Using Monte Carlo simulations, we study the effects of Tomlinson-Harashima precoding on the performance of Bussgang-type blind algorithms and verify our theoretical analysis.

The major contributions of this thesis are:

- A demonstration that a blind equalizer can successfully acquire a THP-encoded signal for both SISO and MIMO systems. We show that THP actually aids blind equalization, as it ensures that the transmitted signal is non-Gaussian.
- An analytical quantification of the effects of THP on the transmitted signal statistics. We derive a novel bound on the kurtosis of the THP-encoded signal.
- An extension of the results from a single-user SISO scenario to multiple users and a MIMO scenario. We demonstrate that our bound and simulated results hold for these more general cases.

Through our work, we have opened the way for a novel application of training sequence-less equalization: to acquire and equalize THP-encoded signals. Using our proposed system, periodic training sequences for a broadcast or point-to-multipoint system can be avoided, improving the bandwidth efficiency of the transceiver. Future modem designs with THP encoding can make use of our advances for bandwidth efficient communication systems.

# ACKNOWLEDGEMENTS

I would sincerely like to thank all those people who played a part in the completion of this thesis. Special thanks to my supervisor, Dr. Lee M. Garth, for his guidance, help and consistent encouragement.

Special thanks to my fellow postgraduate colleagues in the Communications Research Group. I would like to thank you all for the times we spent together, sharing knowledge in all of the meetings. You have made my postgraduate life more colorful and precious.

I would also like to thank my parents for their love and consistent support in the completion of this project and their encouragement of my pursuit of a higher degree and achievements. Lastly, thank you Allah for your mercy, love and grace, being with me all the time.

# CONTENTS

# LIST OF FIGURES

# LIST OF TABLES

# ABBREVIATIONS AND ACRONYMS

**ADSL** Asymmetric Digital Subscriber Line

**ASK** Amplitude Shift Keying

**CMA** Constant Modulus Algorithm

**CSI** Channel State Information

**DFE** Decision Feedback Equalizer

**HDSL** High Bit-Rate Digital Subscriber Line

**i.s.i.** Intersymbol Interference

**i.u.i.** Interuser Interference

**LMS** Least Mean Square

**MIMO** Multi-Input Multi-Output

**MMA** Multi Modulus Algorithm

**MSE** Mean Squared Error

**MMSE** Minimum Mean Squared Error

**QAM** Quadrature Amplitude Modulation

**RCA** Reduced Constellation Algorithm

**SIMO** Single-Input Multiple-Output

**SISO** Single-Input Single-Output

**SNR** Signal-to-Noise Ratio

**THP** Tomlinson-Harashima Precoding

**VDSL** Very High Bit-Rate Digital Subscriber Line

**ZF** Zero-Forcing

# Chapter 1

# INTRODUCTION

## 1.1 BANDWIDTH-EFFICIENT COMMUNICATION SYSTEMS

Bandwidth is one of the precious commodities in modern high-speed communication systems. With widespread broadband adoption the demand for bandwidth is constantly increasing. The greater the bandwidth, the greater the scope is for achieving high speed communications. From a commercial point of view, transmission power and speed are the performance measures for any communication system. Example high speed wireline communications systems are Asymmetric Digital Subscriber Lines (ADSL) and Very High-Bit Rate Digital Subscriber Lines (VDSL) [4]. But, with a training sequence overhead these connections do not exploit their full potential bandwidth. Each time a user is connected to the receiver a training sequence has to be sent. To improve the bandwidth efficiency of the system, this training sequence should be removed.

In recent times the use of multiple antennas at both sides of a communication system has been widely investigated [5]. These so-called multiple-input multiple-output (MIMO) systems can increase the channel capacity and overall transmission rate over conventional single-input single-output (SISO) systems. Example MIMO systems include spatial division multiple access (SDMA) systems in wireless communications and vector coded systems in VDSL wireline communications [6]. But, with the increase of system capacity in MIMO communication systems comes more co-channel interference. To combat this interference, the receiver needs to employ MIMO equalizers. At the cost of bandwidth efficiency, a training sequence-based adaptive equalizer can again separate and recover the multiple signals at the receiver. Again, the removal of training sequences increases the overall bandwidth efficiency.

## 1.2 ADAPTIVE EQUALIZATION

An adaptive equalizer is a crucial receiver component for a bandwidth-efficient communication system. Because of its adaptive nature, it can track the changing channel conditions and then reduce the distorting effects introduced by the channel. In a SISO system, sources of distortion include the lowpass filtering by the channel and additive channel noise. In a MIMO system, another source of distortion is interuser interference (i.u.i.) due to the other users sharing the channel. SISO or MIMO adaptive equalizers try to mitigate these effects and recover the original transmitted data within a certain margin of error.

Conventional trained equalizers require exact knowledge of a portion of the transmitted signal at the receiver. They compare the received data with the training sequence, adapting the equalizer taps to minimize a cost function such as the mean squared error (MSE) [7]. But, for bandwidth-efficient communication systems, particularly broadcast or point-to-multipoint systems, bandwidth is wasted due to the requirement of repeated transmissions of the training sequence. Blind equalizers, on the other hand, are able to start up without a training sequence. Instead of using a training sequence, blind algorithms depend on the higher-order statistics of the transmitted signal.

A widely-used family of blind algorithms is based on the Bussgang algorithm, with a relatively simple cost function which is directly related to the kurtosis of the transmitted signal [8]. The effect of the source distribution on the convergence of Bussgang equalizers has been investigated in [1], [9] – [12]. It has been found that the convergence behavior is consistently good for platykurtic or sub-Gaussian sources [11]. Also, the initial condition for successful convergence of blind equalizers has been found to be dependent on the excess kurtosis of the combined channel-equalizer response [13], [14]. Thus, the distribution of the transmitted signal, characterized by the kurtosis, plays a key role in the performance of Bussgang equalizers. As we will show, by bounding the transmitted signal kurtosis, we can ascertain the potential performance of Bussgang-type algorithms.

Not only are there alternative adaptation algorithms which can be used to eliminate

the training sequence, there are also alternative equalizer structures such as the DFE, which can be used to get rid of the distortions in the received signal. The DFE has a feedforward equalizer, a feedback equalizer and a threshold device. The presence of the two equalizers in the DFE enables it to outperform a conventional linear equalizer in terms of reduced MSE. But, because of its feedback structure, an incorrect decision by the threshold device is fed back, leading to error propagation. When a reverse channel is available, this error propagation can be eliminated by placing the feedback equalizer in the transmitter.

Tomlinson-Harashima Precoding (THP) [15], [16] is a well known method to eliminate error propagation in a DFE. It has been adopted in a wide variety of modern communication systems with reliable feedback channels. In this thesis we study the effect of THP on the source distribution and blind equalization performance. We show that THP bounds the higher-order statistics of the transmitted signal.

## 1.3 THE BLIND-THP SCENARIO

We now consider the combination of blind equalization and THP. Our goal is to study the performance of blind equalization algorithms for Tomlinson-Harashima Precoded (THP) signals in a communication system as shown in Fig. 1.1. Such a system might

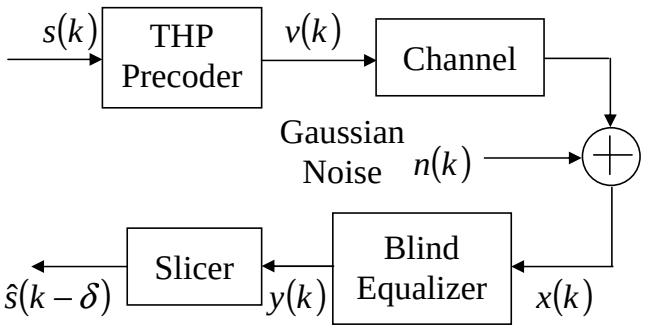


**Figure 1.1** Proposed blind equalization model for THP system

arise in the following scenarios:

1. In modern digital broadcasting or point-to-multipoint systems, such as VDSL, THP can be used to implement spectral masks to prevent egress noise. At the

same time, to increase the overall bandwidth efficiency of the system, receiver set-top boxes can be blindly initialized, instead of using a conventional trained sequence-based adaptive algorithm.[1]

2. Another scenario is in a MIMO-based broadcast system with users blindly trained to the broadcast signal at different times. By using spatial information, a MIMO system can increase the system robustness and capacity. If the precoding is done in the transmitter, then adding a new user using a blind algorithm at the receiver side again increases the bandwidth efficiency of the overall system. In [6] and [18] THP is implemented for MIMO systems, yielding good noise reduction performance.

3. A final scenario is in military applications, where an operative wants to intercept a precoded signal without a training sequence. Blind equalization would enable the interception of an encrypted or scrambled signal.

To characterize the performance of the system shown in Fig. 1.1, in this thesis we consider THP in conjunction with conventional Bussgang-type algorithms. We demonstrate that THP has a bounding effect on the transmitted signal kurtosis, which in turn affects the start-up performance of Bussgang-type algorithms. Unlike previous researchers, we study the effect of THP on the transmitted signal kurtosis. We find that THP bounds the kurtosis of the signal below that of a Gaussian, yielding a sub-Gaussian transmitted signal distribution, which is advantageous for blind equalization. To extend the conventional SISO Bussgang-type algorithms to MIMO systems, the algorithms need to be modified to eliminate the effect of i.u.i. We consider the convergence properties of these modified algorithms for MIMO versions of THP signals. We then use Monte Carlo simulations to verify our kurtosis bounds and to prove that blind equalization is viable for THP systems for a variety of signal constellations for both SISO and MIMO systems.

[1] Researchers have shown that for a twisted-pair cable, if the variation in the cable length is less than 25%, the structure of the cable characteristics from a precoding vantage point remains approximately constant [17].

## 1.4 LITERATURE REVIEW

Many researchers have derived alternative adaptive equalization algorithms to mitigate i.s.i. Lucky [19] was the first to propose a truly adaptive equalization algorithm, using a zero-forcing criterion and the output of the threshold device as the reference signal. This so-called "decision-directed" equalizer can be considered the first blind technique, as it relies on a receiver-generated reference instead of a training sequence. Then, the MSE criterion for adaptive equalization was independently derived by Gersho [20] and Proakis and Miller [21]. The extensively-used Least Mean Square (LMS) algorithm was developed by Widrow and Hoff [22]. A comprehensive tutorial covering all aspects of adaptive equalization can be found in [23]. Generally, these equalizers require exact knowledge of the transmitted signal during the initial adaptation.

Sato first introduced the idea of a training sequence-less equalizer in [24]. Godard [25] then generalized Sato's algorithm to two dimensions and then proposed his own algorithm relying on the higher-order moments of the channel outputs. Treichler and coworkers [26], [27] renamed Godard's algorithm the Constant Modulus Algorithm (CMA), popularizing it by showing its effectiveness. It was not until 1984 that Benveniste and Goursat [28] coined the term *blind equalization*. Unfortunately, CMA suffers from the problem of constellation rotation. Recently, the Multi Modulus Algorithm (MMA) was proposed in [29], which removes this rotation.

But, these blind algorithms only work properly if the transmitted signal is non-Gaussian, as Gaussian signals have higher-order statistics which are zero [8], [10], [30]. So, we cannot directly detect a Gaussian signal using most blind algorithms [9], [10], [31]. The idea of modifying a Gaussian-like signal to make it more non-Gaussian (using precoding) is proposed in [17]. This facilitates the use of adaptive blind equalization for an HDSL-application in the German Telekom subscriber network. But, this modification requires a very highly complex transmitter design. Other problems associated with blind algorithms are the speed of the convergence and the residual mean squared error. A variety of solutions to these problems have been proposed (see e.g. [32],[33]).

Many adaptive equalization structures can be used. From a maximum likelihood estimation vantage point, maximum likelihood sequence estimation, implemented using a

Viterbi detector, is optimal. Unfortunately, the complexity of the detector increases exponentially with the channel length, making it difficult to implement for channels with long impulse responses. A widely-used alternative nonlinear equalization technique is the DFE. The first paper on the DFE was published by Austin [34]. Monsen [35] then optimized the DFE using minimum MSE analysis. For a comprehensive tutorial on the working principle of the DFE see [36]. Its feedback equalizer uses the previously detected symbols to subtract their contribution to the i.s.i. in the symbol which is currently being detected. But, this is contingent on the exact detection of the previous symbols. If incorrect decisions are fed back and subtracted from the present symbol, error propagation results. To get rid of this error propagation, the feedback equalizer can be placed in the transmitter, which is commonly known as pre-equalization.

THP is one such pre-equalization technique, proposed by Tomlinson [15] and Harashima and Miyakawa [16] independently. Other researchers (e.g. Laroia *et al.* [37],[38]) have extended THP to incorporate trellis coding without a loss of coding gain. However, because these extensions make the transmitter structure very complex and difficult to analyze, here we concentrate on THP, which is very simple to implement.

As mentioned before, the combination of THP and blind equalization was previously proposed by Fischer et al. [17], but they did not analyze the performance of Bussgang-type blind algorithms for general THP-shaped source distributions as we do. For the case of MIMO systems, cost-function based blind algorithms have been generalized by Papadias and Paulraj [39] – [41] and Li and Liu [3]. In these papers, they modify the basic Bussgang algorithm to counter the effects of cross-correlation between the transmitted signals. Once again they show that a non-Gaussian signal distribution is necessary for blind equalization in this multiuser scenario.

MIMO versions of THP have been derived for the case when Channel State Information (CSI) is available in the transmitter. In [6] Ginis and Cioffi use the QR decomposition of the channel matrix to derive a matrix form DFE. The feedback matrix of the DFE is then used as the MIMO THP in the transmitter. Similar analysis is done by Fischer et al. in [42], using a multidimensional DFE to implement the precoder. They model the system for a uplink scenario where all the receiver side processing is

transferred to transmitter. In [43], the performance of linear and nonlinear precoding methods for MIMO systems has been analyzed. As a nonlinear precoding method THP is used and it is implemented as a multidimensional DFE. The optimal matrix filters are calculated using Wiener Filter theory. In [44] THP is combined with a successive optimization technique, which uses the singular value decomposition to find the feedforward and feedback filter matrices. It also uses the DFE in the transmitter side.

## 1.5 OUTLINE OF THESIS

The thesis is organized as follows. In Chapter 2, background material on the channel model, decision feedback equalization, Tomlinson-Harashima precoding and Bussgang-type blind algorithms for SISO and MIMO systems are presented. We also review the convergence conditions for MIMO blind equalizers and introduce MIMO versions of Bussgang-type blind algorithms which meet these conditions. In Chapter 3, we derive the decision feedback equalizer tap weights to use in the transmitter of a THP system for both SISO and MIMO systems and analytically bound the kurtosis of a THP-encoded signal. In Chapter 4, we verify our analytical results using Monte Carlo simulations. In Chapter 5, we conclude with the core results of this thesis and indicate possible topics for future research.

# Chapter 2

# BACKGROUND

In this chapter, we review in detail the decision feedback equalizer (DFE), the Tomlinson-Harashima precoder (THP) and Bussgang-type blind algorithms. We consider both SISO and MIMO systems. In Sections 2.1 and 2.2 we give general descriptions of the channel model and the DFE for SISO systems. The same descriptions for MIMO systems are given in Section 2.3. SISO and MIMO versions of THP are discussed in Section 2.4. Finally, in Sections 2.5 and 2.6 we review Bussgang-type blind algorithms for SISO and MIMO systems.

## 2.1 SISO CHANNEL MODEL

In a communication system the transmitted signal passes through an inter-symbol interference (i.s.i.) producing channel. In addition, the signal is corrupted by noise. Generally, the noise is assumed to be additive, white, Gaussian and independent of the transmitted signal. Such a communication system is shown in Fig. 2.1. After Nyquist

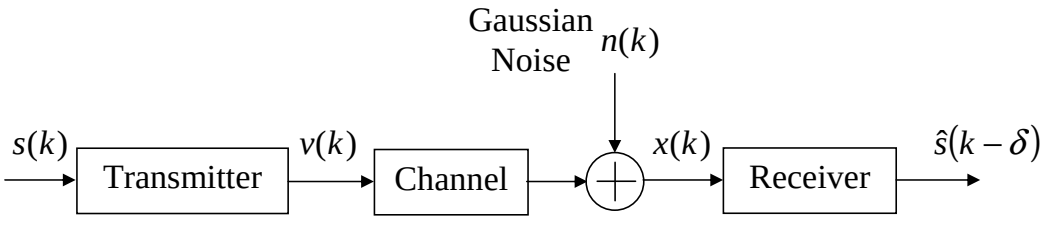


**Figure 2.1** General model of a communication system

sampling, if we group the discrete-time observations at the receiver into a length $N_f$

vector $\boldsymbol{x}$, the effects of the channel can be represented using

$$\boldsymbol{x} = \boldsymbol{H}\boldsymbol{s} + \boldsymbol{n}, \tag{2.1}$$

where

$$\begin{aligned}
\boldsymbol{H} &= \begin{bmatrix} h_1 & h_2 & \cdots & h_L & 0 & \cdots & 0 \\ 0 & h_1 & h_2 & \cdots & h_L & 0 & 0 \\ 0 & 0 & \ddots & \ddots & \ddots & \ddots & 0 \\ 0 & \cdots & 0 & h_1 & h_2 & \cdots & h_L \end{bmatrix} \\
\boldsymbol{x} &= [x(k) \quad x(k-1) \ \cdots \ x(k-N_f+1)]^T \\
\boldsymbol{s} &= [s(k) \quad s(k-1) \ \cdots \ s(k-N_f+1-L+1)]^T \\
\boldsymbol{n} &= [n(k) \quad n(k-1) \ \cdots \ n(k-N_f+1)]^T
\end{aligned} \tag{2.2}$$

and $\boldsymbol{H}$ is the $N_f$ by $N_f + L - 1$ channel convolution matrix, and its elements are the channel impulse response of length $L$. Here, $(\cdot)^T$ denotes the transpose. Vector $\boldsymbol{n}$ contains the mean-zero i.i.d. noise samples with variance $\sigma_n^2$, which are assumed to be independent of the transmitted symbols in $\boldsymbol{s}$. The transmitted symbols are assumed to be i.i.d. with mean zero and variance $\sigma_s^2$.

## 2.2 DECISION FEEDBACK EQUALIZATION AND PRE-EQUALIZATION

To remove the i.s.i. and noise, an adaptive equalizer tries to learn and invert the channel. A widely-used structure is the decision feedback equalizer (DFE) shown in Fig. 2.2, which comprises of a feedforward filter, a feedback filter and a threshold device. In the DFE the sequence of observations to be equalized is applied to the feedforward filter, and the decisions made on previously detected symbols are applied to the feedback filter. The function of the feedback filter is to subtract out that portion of the i.s.i. produced by previously detected symbols (often called precursors) from the estimates of the future samples [35].

Let the feedforward and feedback tap weights of the DFE be represented respectively

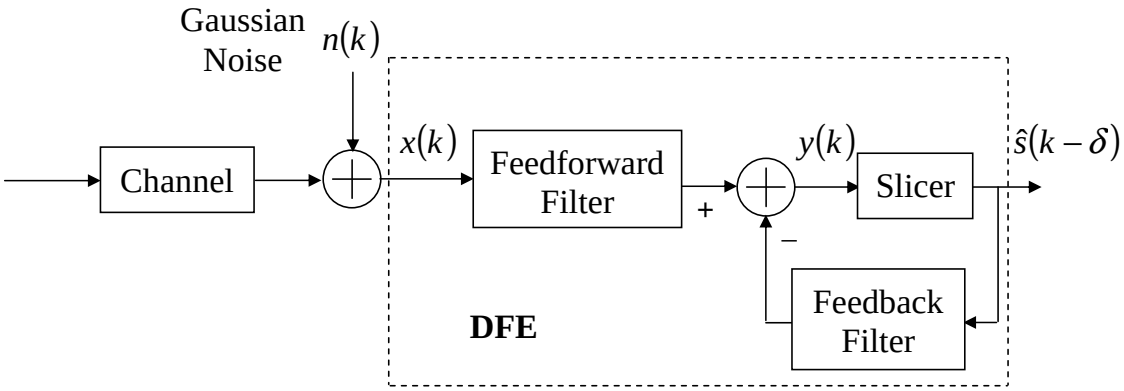


**Figure 2.2** Decision Feedback Equalizer

by vectors

$$\boldsymbol{f} = [f_1\ f_2\ \cdots\ f_{N_f}]^T \qquad \boldsymbol{b} = [b_1\ b_2\ \cdots\ b_{N_b}]^T. \tag{2.3}$$

At time $k$, the feedforward filter contains the $N_f$ channel observations, denoted by $\boldsymbol{x}$. During equalizer training, instead of using the slicer outputs, the actual mean-zero i.i.d. transmitted symbols $s(k)$ corresponding to the equalizer outputs are fed into the feedback filter. Thus, the DFE tries to recover the symbol $s(k-\delta)$ with propagation delay $\delta$, and hence the input to the feedback filter is $\boldsymbol{s}_B = [s(k-\delta-1)\ s(k-\delta-2)\ \cdots\ s(k-\delta-N_b)]^T$.

Now, the feedforward and feedback data vectors and weight vectors of the DFE can combined as

$$\boldsymbol{z} = \begin{bmatrix} \boldsymbol{x} \\ -\boldsymbol{s}_B \end{bmatrix} \qquad \boldsymbol{w} = \begin{bmatrix} \boldsymbol{f} \\ \boldsymbol{b} \end{bmatrix}, \tag{2.4}$$

yielding slicer input $y(k) = \boldsymbol{w}^H \boldsymbol{z}$, where $(\cdot)^H$ represents the Hermitian transpose. The feedback filter will work well provided that the decisions made by the slicer are correct. However, if the slicer starts to give wrong estimates, then the feedback filter starts to propagate errors, and, because of the feedback property, this error propagation starts to accumulate and results in instability. In the presence of noise, even the optimum

tap weights of the DFE cannot avoid error propagation.

Wiener filter theory can be used to derive the optimum tap weights by minimizing the mean squared error (MSE) difference between the desired signal and the received signal [7]. Statistically, the Wiener filter depends on the autocorrelation matrix and cross-correlation vector of the transmitted signal. For a given integer propagation delay $\delta$, the Wiener filter taps can be calculated using the formula

$$\boldsymbol{w}_\delta = \boldsymbol{R}_\delta^{-1} \boldsymbol{p}_\delta. \tag{2.5}$$

The optimum tap weights correspond to the delay $\delta$ for which the MSE is the minimum, which is found using

$$\delta_{\text{opt}} = \arg \min_{1 \le \delta \le N_f + L - 1 - N_b} \sigma_s^2 - \boldsymbol{p}_\delta^H \boldsymbol{R}_\delta^{-1} \boldsymbol{p}_\delta, \tag{2.6}$$

where $\boldsymbol{R}_\delta$ denotes the autocorrelation matrix

$$\boldsymbol{R}_\delta = \mathrm{E}\{\boldsymbol{z}\, \boldsymbol{z}^H\} = \begin{bmatrix} \mathrm{E}\{\boldsymbol{x}\, \boldsymbol{x}^H\} & -\mathrm{E}\{\boldsymbol{x}\, \boldsymbol{s}_B^H\} \\ -\mathrm{E}\{\boldsymbol{s}_B\, \boldsymbol{x}^H\} & \mathrm{E}\{\boldsymbol{s}_B\, \boldsymbol{s}_B^H\} \end{bmatrix}, \tag{2.7}$$

and $\boldsymbol{p}_\delta$ is the cross-correlation vector

$$\boldsymbol{p}_\delta = E\{\boldsymbol{z}\, s^*(k-\delta)\} = \begin{bmatrix} \boldsymbol{H} E\{\boldsymbol{s}\, s^*(k-\delta)\} \\ -E\{\boldsymbol{s}_B\, s^*(k-\delta)\} \end{bmatrix}. \tag{2.8}$$

As both the symbols and noise are i.i.d., it can be shown that

$$\begin{aligned} &\mathrm{E}\{\boldsymbol{x}\, \boldsymbol{x}^H\} = \sigma_s^2 \boldsymbol{H} \boldsymbol{H}^H + \sigma_n^2 \boldsymbol{I}_{N_f} \\ &\mathrm{E}\{\boldsymbol{s}_B \boldsymbol{s}_B^H\} = \sigma_s^2 \boldsymbol{I}_{N_b} \\ &\mathrm{E}\{\boldsymbol{x}\, \boldsymbol{s}_B^H\} = \boldsymbol{H}\, \mathrm{E}\{\boldsymbol{s}\, \boldsymbol{s}_B^H\} = \boldsymbol{H} \begin{bmatrix} \boldsymbol{O}_{\delta \times N_b} \\ \sigma_s^2 \boldsymbol{I}_{N_b} \\ \boldsymbol{O}_{(N_f + L - 1 - \delta - N_b) \times N_b} \end{bmatrix}, \end{aligned} \tag{2.9}$$

where $\boldsymbol{I}_M$ denotes the $M \times M$ identity matrix and $\boldsymbol{O}_{K \times J}$ is a $K \times J$ zero matrix. Using

MATLAB notation, we can write

$$\mathrm{E}\{\boldsymbol{x}\, \boldsymbol{s}_B^H\} = \sigma_s^2\, \boldsymbol{H}(:, \delta + 1 : \delta + N_b), \tag{2.10}$$

where $\boldsymbol{H}(:, i : j)$ denotes the $i$-th through $j$-th rows of $\boldsymbol{H}$. Similarly, because of the independence of the symbols and noise, the cross-correlation vector $\boldsymbol{p}_\delta$ has the form

$$\boldsymbol{p}_\delta = \begin{bmatrix} \sigma_s^2 \boldsymbol{H}(:, \delta) \\ \mathbf{0}_{N_b \times 1} \end{bmatrix}. \tag{2.11}$$

After the training is completed, assuming a reliable reverse channel exists, a practical way of stopping error propagation in the DFE is to shift the feedback filter from the receiver side to the transmitter side, which is possible due to the linearity of the overall transceiver system and channel model. This results in the equalization system shown in Fig. 2.3. If we retain the same symbol power levels for $s(k)$, linear pre-equalization performs equivalently to linear equalization at the receiver [45]. If, however, we normalize the transmitted power, then the performance of the precoded system is degraded. This is because the pre-equalization filter typically causes signal power enhancement at the transmitter power amplifier. One way to avoid this signal power enhancement without degrading the system performance is to introduce a limiter or non-linearity into the feedback loop. This is known as precoding, which we discuss further in Section 2.4.

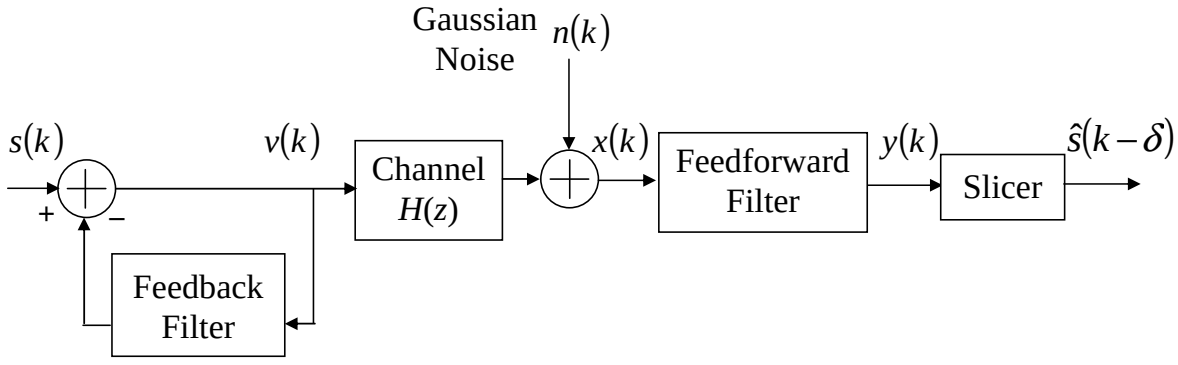


**Figure 2.3** Pre-equalization at the transmitter side

## 2.3 MIMO CHANNEL MODEL AND DFE

Now let us consider a more general MIMO system with $N_T$ transmitters and $N_R$ receivers. The channel between each transmitter and receiver is assumed to be a complex-valued baseband channel. The MIMO channel model and corresponding DFE are now presented in Sections 2.3.1 and 2.3.2.

### 2.3.1 MIMO Channel Model

Figure 2.4 shows a block diagram of our $N_T \times N_R$ MIMO communication model. Using

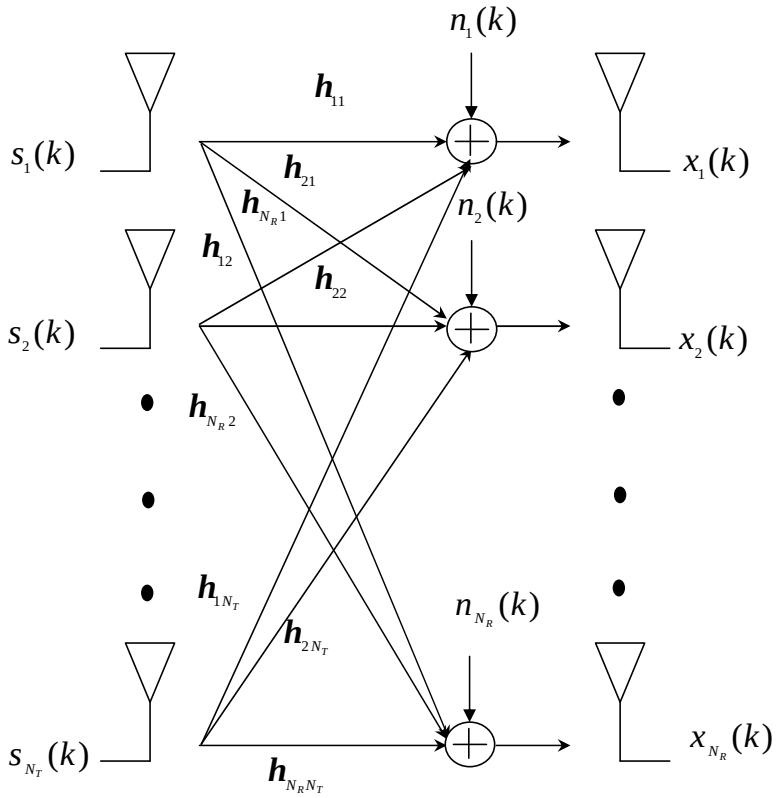


**Figure 2.4** Block diagram of MIMO channel model

the notation of [46], the channel output at the $j$-th receiver ($1 \le j \le N_R$) at time $k$ is

$$x_j(k) = \sum_{i=1}^{N_T} \sum_{m=0}^{\ell_i - 1} h_{ji}^m \, s_i(k-m) + n_j(k), \tag{2.12}$$

where $h_{ji}^{m}$ represents the channel impulse response between the $i$-th input and $j$-th output, with memory $(\ell_i - 1)$. Similar to the SISO model, the symbols from the $i$-th transmitter $s_i(k), i = 1, \ldots, N_T$, are assumed to be i.i.d. with zero mean and variance $\sigma_s^2$. The additive noise at the $j$-th receiver $n_j(k)$ is assumed to be Gaussian, i.i.d. with zero mean and variance $\sigma_n^2$. The signal and noise are again assumed to be mutually independent.

The channel impulse response can be represented as a vector denoted by $\boldsymbol{h}_{ji} = [h_{ji}^{0} \quad h_{ji}^{1} \quad \cdots \quad h_{ji}^{(\ell_i - 1)}]$. Now, at a time $k$ all the channel outputs can be grouped in a vector to represent the channel output in the form

$$\boldsymbol{x}(k) = \sum_{m=0}^{L-1} \boldsymbol{H}_m \, \boldsymbol{s}(k-m) + \boldsymbol{n}(k), \tag{2.13}$$

where $\boldsymbol{H}_m$ is the $N_R \times N_T$ MIMO channel matrix corresponding to the $m$-th lag of the MIMO channel impulse response of the form

$$\boldsymbol{H}_m = \begin{bmatrix} h_{11}^{m} & h_{12}^{m} & \cdots & h_{1N_T}^{m} \\ \vdots & \ddots & \vdots & \\ h_{N_R1}^{m} & h_{N_R2}^{m} & \cdots & h_{N_RN_T}^{m} \end{bmatrix} \tag{2.14}$$

and $\boldsymbol{s}(k)$ is the $N_T \times 1$ input vector at time $k$. Here $L = \max_i \ell_i$ denotes the maximum length of all the component channel impulse responses.

### 2.3.2 MIMO DFE

The corresponding MIMO DFE, comprising of feedforward filters, feedback filters and threshold devices, can be used to remove the i.s.i. and i.u.i. in a MIMO channel. Again, let $N_f$ and $N_b$ represent the length of each of the feedforward and feedback filters, respectively. We define component matrix $\boldsymbol{F}_m$ to contain the $N_R \times N_T$ feedforward tap weights for lag $m$ and $\boldsymbol{B}_m$ to contain the $N_T \times N_T$ feedback tap weights for lag $m$.

The matrix forms of $\boldsymbol{F}_m$ and $\boldsymbol{B}_m$ are

$$\boldsymbol{F}_m = \begin{bmatrix} f_{11}^m & \cdots & f_{N_T 1}^m \\ \vdots & \ddots & \vdots \\ f_{1N_R}^m & \cdots & f_{N_T N_R}^m \end{bmatrix}, \qquad \boldsymbol{B}_m = \begin{bmatrix} b_{11}^m & \cdots & b_{N_T 1}^m \\ \vdots & \ddots & \vdots \\ b_{1N_T}^m & \cdots & b_{N_T N_T}^m \end{bmatrix}, \tag{2.15}$$

where each $f_{ij}^m$ denotes the $m$-th tap of the feedforward filter for the $i$-th transmitter and $j$-th receiver, and each $b_{ij}^m$ denotes the $m$-th tap of the feedback filter between the $i$-th and $j$-th transmitters. Alternatively, we can group all of the tap weights for a particular $i$-th transmitter and $j$-th receiver (or transmitter) in the vectors

$$\begin{aligned} \boldsymbol{f}_{ij} &= [f_{ij}^0 \quad f_{ij}^1 \ \cdots \ f_{ij}^{N_f-1}]^T, \qquad 1 \le i \le N_T, \qquad 1 \le j \le N_R \\ \boldsymbol{b}_{ij} &= [b_{ij}^0 \quad b_{ij}^1 \ \cdots \ b_{ij}^{N_b-1}]^T, \qquad 1 \le i, j \le N_T. \end{aligned} \tag{2.16}$$

Now, the equalizer output can be expressed as

$$\boldsymbol{y}(k) = \sum_{m=0}^{N_f-1} \boldsymbol{F}_m^H \boldsymbol{x}(k-m) - \sum_{m=0}^{N_b-1} \boldsymbol{B}_m^H \boldsymbol{s}_B(k-m), \tag{2.17}$$

where $\boldsymbol{s}_B$ is the input vector to the feedback filter. During equalizer training, instead of the slicer outputs, the corresponding transmitted data symbols, $s_i(k), i = 1, \ldots, N_T$, again are fed into the feedback filters. The input vector $\boldsymbol{s}_B$ is filled with the transmitted data symbols and has the form

$$\boldsymbol{s}_B(k) = [s_1(k-\delta_1) \quad s_2(k-\delta_2) \ \cdots \ s_{N_T}(k-\delta_{N_T})]^T. \tag{2.18}$$

The MIMO DFE tries to recover all the independent transmitted symbols with propagation delay $\delta_i$, which lies in the interval $0 \le \delta_i \le N_f + L - 1$ [46]. To find the delay for each transmitter, we send an impulse from each transmitter. Each impulse passes through $N_R$ different paths before reaching the receiver. For example, for the MIMO DFE structure for a $2 \times 3$ system (Fig. 2.5), if transmitter 1 sends an impulse, then it reaches the corresponding receiver having travelled over three different channels. The first path is between $\boldsymbol{h}_{11}$ and $\boldsymbol{f}_{11}$, the second path is between $\boldsymbol{h}_{12}$ and $\boldsymbol{f}_{21}$ and the

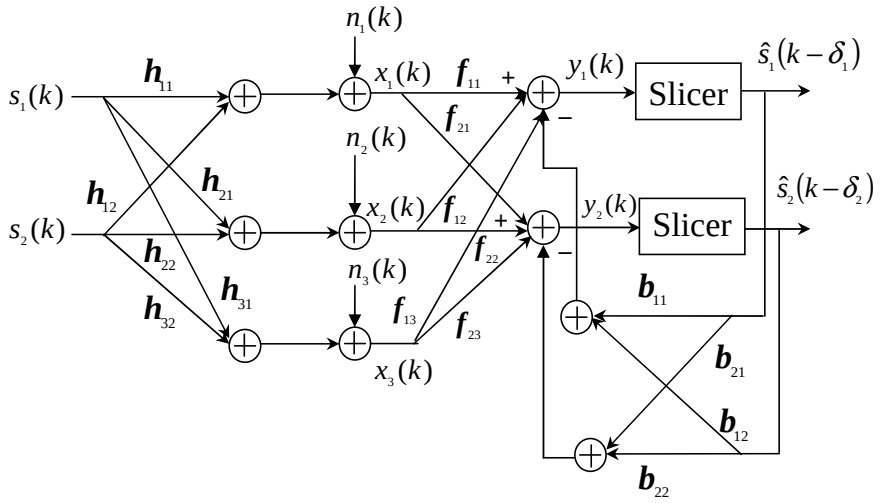


**Figure 2.5** Decision Feedback Equalizer for a 2 × 3 system

third path is between $\boldsymbol{h}_{13}$ and $\boldsymbol{f}_{31}$. The net delay for transmitter 1 is then computed using the combined channel-equalizer response due to the three channels.

Similar to the SISO case, assuming a reliable reverse channel, the feedback filters of the MIMO DFE can be transferred to the transmitter to mitigate the error propagation problem. But this causes signal power enhancement at the transmitter side. Again, MIMO precoding can be used to reduce this enhancement.

## 2.4 TOMLINSON-HARASHIMA PRECODING

In a THP system the equalization is done in the transmitter using an inverse modulo filter. Therefore, error correction coding techniques can be applied in the same way as for channels without i.s.i. Note that to construct the optimal modulo filter, the channel transfer function needs to be known at the transmitter both for SISO and MIMO systems.

Figure 2.6 is a general representation of a SISO THP system. The modulo adder basically wraps around the signal constellation so that the signal does not expand infinitely, increasing the transmit power. If the data signal is drawn from an $M$-point one-dimensional PAM signal set $A = \{\pm 1, \pm 3, \ldots, \pm(M-1)\}$, for even $M$, then the modulo adder makes sure that the signal set does not go beyond the interval [-$M$, +$M$).

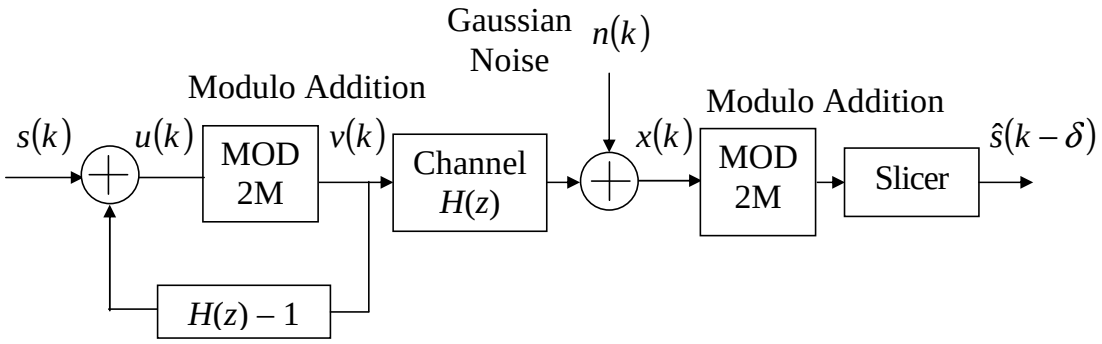


**Figure 2.6** SISO Tomlinson-Harashima Precoder

Figure 2.7 shows an example plot of the function employed by the modulo adder for $M = 4$. Hence, the modulo adder over a fixed interval of, say, [-$M$, +$M$) implements

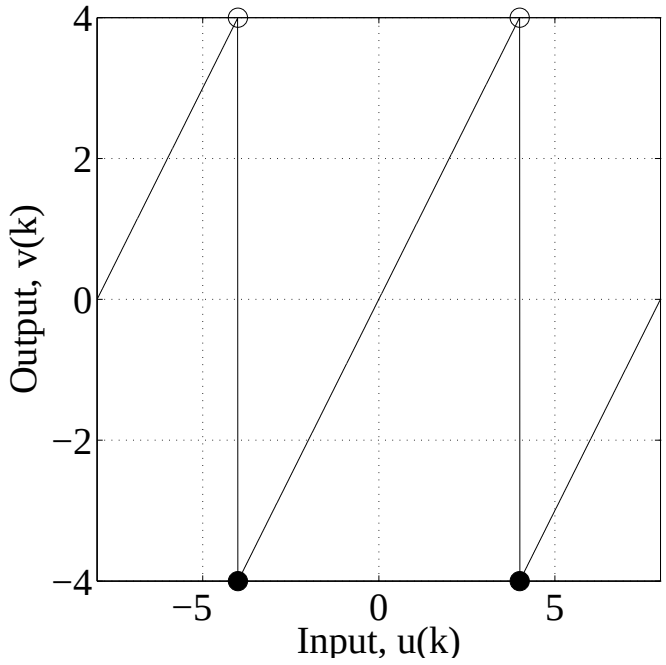


**Figure 2.7** Output vs. input for the modulo adder

the following algorithm:

1. If the result of the summation, $u(k)$ is greater than $M$, $2M$ is deducted from it until it is less than $M$.

2. If the result of the summation, $u(k)$ is less than -$M$, $2M$ is added to it until it is greater than or equal to $-M$.

If the data symbols are drawn from an $M$-ary square QAM signal set $A = \{a+j\,b \,|\, a, b \in \pm 1, \pm 3, \cdots \pm(\sqrt{M}-1)\}$, then the modulo adder makes sure that the real and imaginary parts of the precoded symbols lie in the interval [$-\sqrt{M}$, $+\sqrt{M}$). Due to the modulo operation, all the points spaced by integer multiples of $2\sqrt{M}$ in real or imaginary part represent the same data.

The concept of Tomlinson-Harashima precoding (THP) for SISO channels can be easily extended to MIMO channels. Figure 2.8 shows a generalized MIMO THP system for a zero-forcing (ZF) system. Similar to the SISO case, the direct realization of THP

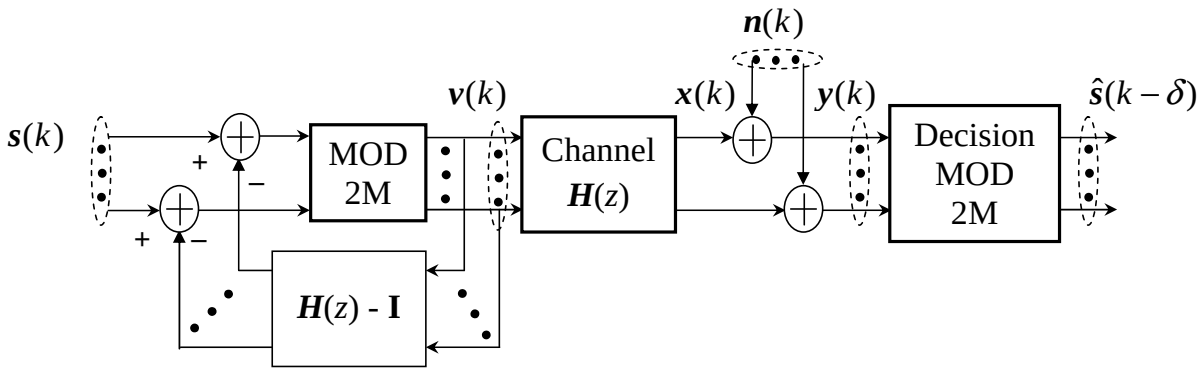


**Figure 2.8** MIMO Tomlinson-Harashima Precoder

requires advanced knowledge of the Channel State Information (CSI) matrix $\boldsymbol{H}(z)$.

One result of implementing SISO or MIMO THP is the input data is scrambled into a pseudorandom sequence [16]. This scrambling spreads the frequency spectrum of the data, and so reduces the intermodulation effects, but it colors the data unlike a conventional scrambler which has a whitening effect.

As the input data sequence is modified because of the modulo addition, the receiver needs to apply the same modulo operation to the received data to retrieve the original transmitted symbol. Hence, the received sequence is passed through the modulo adder based on the same algorithm as in the transmitter before it is passed through the slicer.

## 2.5 BLIND EQUALIZATION

Normally, for the equalizer to "learn" the channel characteristics the transmitter sends a training sequence to the receiver, interrupting the normal transmission mode periodically as the channel changes or new users join a point-to-multipoint system. But, in a broadcast network or point-to-multipoint network a periodic training sequence wastes valuable bandwidth for all of the users. Bandwidth is very costly, so its efficient utilization is one of the prime factors in designing modern transmission systems.

A trained equalizer is adapted to align the output of the equalizer due to a particular transmitted symbol with the symbol itself, and the final equalizer taps attempt to produce the closest matching (i.e., when the difference between the equalizer output and the desired symbol is minimum). Various kinds of algorithms such as the Least Mean Square (LMS), Normalized Least Mean Square (NLMS) and Recursive Least Squares (RLS) algorithms are available to minimize the mean squared error or the least squares fit of the data to provide the best equalizer output [7].

By eliminating the need for a periodic training sequence, blind equalization reduces bandwidth wastage. A blind equalizer is "blind" because it does not require any training sequence of predetermined symbols; all it utilizes are the statistical characteristics of the transmitted signal. Based on these statistics, the equalizer recovers the transmitted signal. By matching certain properties of the transmitted signal derived from its higher-order statistics, many cost function-based algorithms have been developed including the Sato algorithm, Godard-Constant Modulus Algorithm (CMA), Multi Modulus Algorithm (MMA) and Reduced Constellation Algorithm (RCA) [8]. Each algorithm opens the "eye" of the blind equalizer, mitigating the channel distortion of the transmitted signal.

The CMA cost function is of the form [26]:

$$\mathrm{CF}_{\mathrm{CMA}} = \mathrm{E}\{[|y(k)|^2 - R_c^2]^2\}, \qquad \text{where } R_c^2 = \frac{\mathrm{E}\{|s(k)|^4\}}{\mathrm{E}\{|s(k)|^2\}}. \tag{2.19}$$

Here, $y(k)$ is the output of the equalizer, and $s(k)$ is the data symbol. This cost function can be interpreted as fitting the output data constellation of the equalizer to a circle

of radius $R_c$, shown in Fig. 2.9.

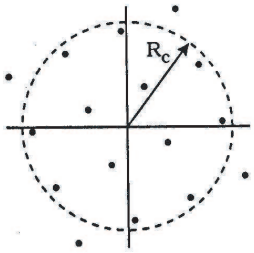


**Figure 2.9** Graphical representation of CMA from [1]

Similarly, the MMA cost function is:

$$\mathrm{CF_{MMA}} = \mathrm{E}\{[y_r^2(k) - R_m^2]^2 - [y_i^2(k) - R_m^2]^2\}, \quad \text{where } R_m^2 = \frac{\mathrm{E}\{a^4(k)\}}{\mathrm{E}\{a^2(k)\}} = \frac{\mathrm{E}\{b^4(k)\}}{\mathrm{E}\{b^2(k)\}}. \tag{2.20}$$

Here subscripts $r$ and $i$ indicate the real and imaginary parts of of the equalizer output $y(k)$, and $a(k)$ and $b(k)$ are the real and imaginary parts of the data symbol $s(k)$. We assume that $\mathrm{E}\{a^n(k)\} = \mathrm{E}\{b^n(k)\}$. The cost function can be interpreted as fitting the output data constellation of the equalizer to a square with side lengths $2R_m$. Fig. 2.10 shows its graphical representation.

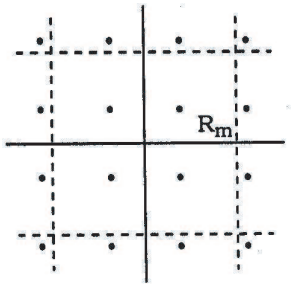


**Figure 2.10** Graphical representation of MMA from [1]

Finally, the RCA cost function is defined as:

$$\mathrm{CF_{RCA}} = \mathrm{E}\{|y(k) - R_r \,\mathrm{csgn}[y(k)]|^2\}, \qquad \text{where } R_r^2 = \frac{\mathrm{E}\{a^2(k)\}}{\mathrm{E}\{|a(k)|\}} \tag{2.21}$$

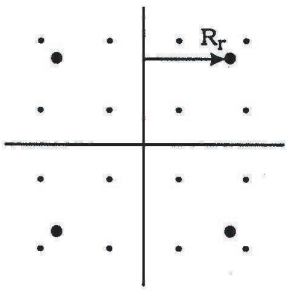


**Figure 2.11** Graphical representation of RCA from [1]

with $\text{csgn}(y) = \text{csgn}(y_r + jy_i) = \text{sgn}(y_r) + j\,\text{sgn}(y_i)$, corresponding to fitting the output data constellation of the equalizer to a reduced four-point square constellation. Its graphical representation is presented in Fig. 2.11. The equalizer tap weights can be updated using a stochastic gradient-type recursion [1]. Note that these Bussgang-type algorithms produce a sign ambiguity in the decoded signal. Thus, to mitigate this problem, we assume that the transmitted signal is differentially modulated.

## 2.6 BLIND EQUALIZATION FOR MIMO SYSTEMS

The same algorithms can be used for MIMO systems. But, MIMO channel separation is crucial for successful reception of the transmitted signals. The condition of distortionless reception for a SISO system requires that the $z$-transform of the system impulse response has no zeros on the unit circle [8]. The same condition can be extended to find necessary and sufficient conditions for the identifiability of MIMO channels [3], [47]. We review these conditions in the following sections.

### 2.6.1 Condition for MIMO Channel Identification

Figure 2.12 shows an $N_T \times N_R$ MIMO system with a linear equalizer at the receiver. Setting the channel noise to zero, the linear equalizer satisfies the condition of distortionless reception when

$$\boldsymbol{F}(z)\boldsymbol{H}(z) = \boldsymbol{I}_{N_T}, \tag{2.22}$$

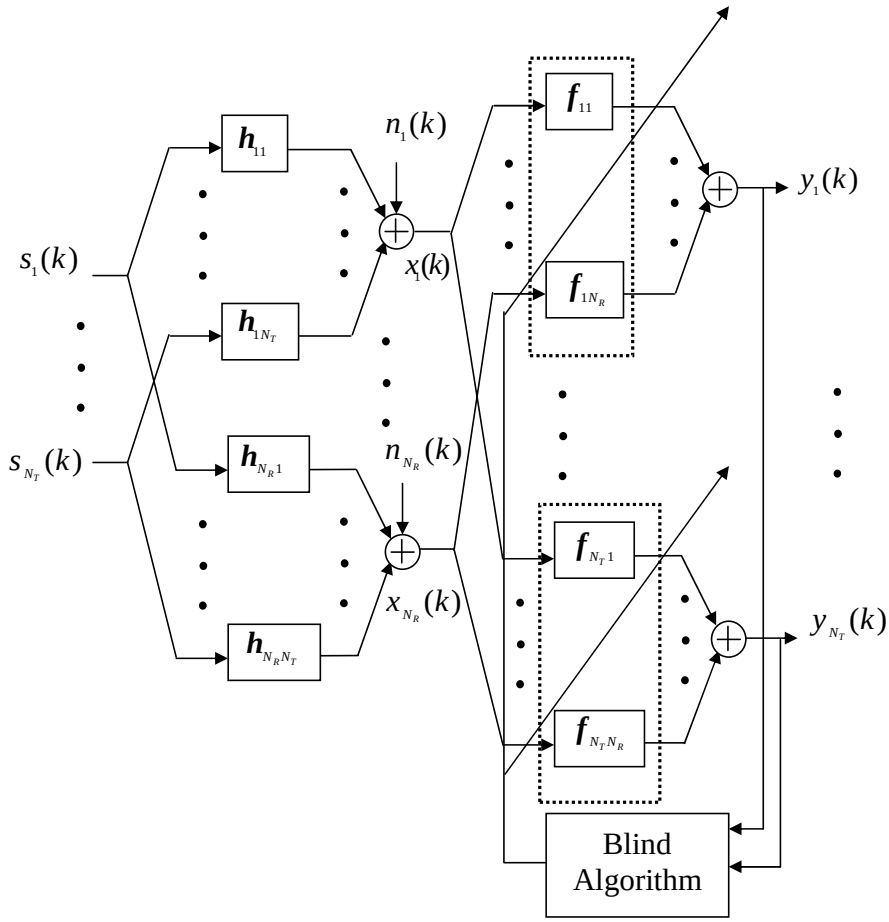


**Figure 2.12** MIMO system with linear equalizer

where $\boldsymbol{F}(z)$ and $\boldsymbol{H}(z)$ represent the $z$-transforms of the equalizer and channel matrix respectively, and $\boldsymbol{I}_{N_T}$ is an $N_T \times N_T$ identity matrix. This condition yields a bounded-input bounded-output (BIBO) stable equalizer at the receiver. Mathematically, this BIBO zero-forcing receiver has the form [3]

$$\boldsymbol{F}(e^{j\omega}) = [\boldsymbol{H}^H(e^{j\omega})\boldsymbol{H}(e^{j\omega})]^{-1}\boldsymbol{H}^H(e^{j\omega}), \quad \text{for} \quad N_R \geq N_T. \tag{2.23}$$

Therefore, $\boldsymbol{H}^H(e^{j\omega})\boldsymbol{H}(e^{j\omega})$ has to be nonsingular for all $\omega \in [-\pi, \pi]$. In other words, a MIMO channel is identifiable if $\boldsymbol{H}(e^{j\omega})$ is of full (column) rank for all $\omega \in [-\pi, \pi]$. This implies that the number of system outputs is no less than the number of system inputs, $N_R \geq N_T$.

### 2.6.2 Initial Convergence Condition for MIMO Blind Equalizer

In this thesis, we consider Bussgang-type algorithms in particular to update the MIMO equalizer. As already mentioned, these algorithm use the higher-order moments for the recovery of the source data. For the linear equalizer of Fig. 2.12 the equalizer output can be expressed as

$$y_j(k) = \sum_{i=1}^{N_T} \sum_{\ell=-\infty}^{\infty} s_i(\ell) c_{ij}(k-\ell), \quad j = 1, \ldots, N_T, \tag{2.24}$$

where $c_{ij}$ is the combined channel-equalizer system response, corresponding to the $i$-th transmitted signal and $j$-th output of the equalizer. The combined response is related to $h_{ji}$ and $f_{ij}$ by

$$c_{ij}(k) = \sum_{m=1}^{N_R} f_{jm}(k) \star h_{mi}(k), \tag{2.25}$$

where $\star$ denotes the convolution. This combined response can be used in expressing the Bussgang-type cost functions. For the MIMO channel model, we only consider the CMA algorithm. Analogous expressions can be derived both for MMA and RCA cost functions.

The CMA cost function for the MIMO system can be expressed as

$$\mathrm{CF}_{\mathrm{CMA}}^{\mathrm{MIMO}} = \mathrm{E}\left\{ \sum_{j=1}^{N_T} [|y_j(k)|^2 - R_c^2]^2 \right\}, \quad \text{where} \quad R_c^2 = \frac{\mathrm{E}\{|s_i(k)|^4\}}{\mathrm{E}\{|s_i(k)|^2\}} = \frac{m_{4s}}{m_{2s}}, \tag{2.26}$$

and $m_{4s}$ and $m_{2s}$ represent the fourth and second absolute moments of the transmitted signal. From (2.24) and (2.26) the CMA cost function for the equalizer output $y_j$ can be written as a function of $c_{ij}$ leading to

$$\begin{aligned} \mathrm{CF}_{\mathrm{CMA}}^{\mathrm{MIMO}} = \sum_{j=1}^{N_T} \Bigg[ & -(\kappa_G\, m_{2s}^2 - m_{4s}) \sum_{i,k} |c_{ij}(k)|^4 + \kappa_G\, m_{2s}^2 \left\{ \sum_{i,k} |c_{ij}(k)|^2 \right\}^2 \\ & - \kappa_G\, m_{4s} \sum_{i,k} |c_{ij}(k)|^2 + \frac{m_{4s}^2}{m_{2s}^2} \Bigg]. \end{aligned} \tag{2.27}$$

where kurtosis, $\kappa_\times$ for a particular signal $\times$ is defined as the ratio of the fourth moment

to the square of the second moment of the input signal, written as:

$$\kappa_{\times} = \frac{\mathrm{E}\{|\times(k)|^4\}}{[\mathrm{E}\{|\times(k)|^2\}]^2}. \tag{2.28}$$

In (2.27) the kurtosis is specifically for a Gaussian signal with $\kappa_G = 3$ for real Gaussian signals and $\kappa_G = 2$ for complex Gaussian signals.[1]

So, if the MIMO system satisfies the distortionless reception condition (2.22) and the length of the equalizer is double-infinite, then using Foschini's argument [5], in [3] it is shown that the minimum points of cost function (2.27) are

$$|c_{ij}[k]|^2 = \delta[k-k_d, i-i_0, j-j_0], \quad \text{for some integers} \quad k_d, \quad i_0 \quad \text{and} \quad j_0. \tag{2.29}$$

The Dirac delta $\delta[k,i,j]$ is defined as

$$\delta[k,i,j] = \begin{cases} 1, & \text{if } k=i=j=0 \\ 0, & \text{otherwise.} \end{cases} \tag{2.30}$$

In [3] a condition for satisfactory equalizer convergence is derived, requiring the following definitions:

- The **Attainable Set** for a given equalizer is:

$$C_a = \{\boldsymbol{c} : c_{ij}(k) = \sum_{m=1}^{N_R} \sum_{\ell} h_{mi}(k-\ell) f_{im}(\ell), \\ \sum_{\ell} |f_{ij}(\ell)| < \infty\}, \quad j = 1, \ldots, N_T. \tag{2.31}$$

- The **Unique Global Minimum Set Cone** is:

$$C_{i,j,k} = \{\boldsymbol{c} : |c_{ij}(k)| > |c_{i'j'}(k')| \quad \text{for all} \quad i \neq i' \quad \text{or} \quad j \neq j' \quad \text{or} \quad k \neq k' \\ \text{and} \sum_{i,j,k} |c_{ij}(k)| < \infty\}. \tag{2.32}$$

[1] In [3], the CMA cost function is found only for a single transmitter, whereas we generalize the expression in (2.27) to accommodate any number of transmitters.

- The **Boundary of** $C_{i,j,k}$ is:

$$B_{i,j,k} = \{\boldsymbol{c} : |c_{ij}(k)| = |c_{i'j'}(k')| \quad \text{for some} \quad i \neq i' \quad \text{or} \quad j \neq j' \quad \text{or} \quad k \neq k' \quad \text{and} \sum_{i,j,k} |c_{ij}(k)| < \infty\}. \tag{2.33}$$

Using these definitions, Li and Liu prove the following theorem:

**Theorem 1** *If the initial equalizer parameter weights are such that the initial system response vector* $\boldsymbol{c}^o \in C_a \cap C_{i,j,k}$ *and its output satisfies the kurtosis condition*

$$\frac{\gamma_y}{\gamma_s} > 0.5, \tag{2.34}$$

*where*

$$\gamma_\times = \frac{m_{4\times}}{m_{2\times}^2} - \kappa_G \tag{2.35}$$

*is the excess kurtosis, then for a sufficiently small step size, the equalizer will cause* $\boldsymbol{c}$ *to converge to a minimum point inside* $C_a \cap C_{i,j,k}$*. (For the case of a complex random variable (2.35) holds if* $\mathrm{E}\{\times^2\} = 0$*.)*

Hence, the initial response vector $\boldsymbol{c}^o$ has a crucial role in the initial performance of the blind equalizer. Note that condition (2.34) is related to our previous statement that Bussgang-type blind algorithms only work well for non-Gaussian signals. Also, under the stated convergence conditions CMA cost function (2.27) will converge to a setting such that each equalizer output $y_j(k)$, $j = 1, \ldots, N_T$, is possibly a shifted and rotated version of the transmitted symbol $s_i(k)$, $i = 1, \ldots, N_T$.

### 2.6.3 Modified Bussgang Algorithms for MIMO Systems

Whether an equalizer based on cost function (2.27) can recover all of the transmitted signals depends on the channel parameters. In a SISO system, the transmitted symbol is corrupted by the noise and its own postcursors and precursors. But, in MIMO systems each transmitted symbol is also corrupted by the other transmitted symbols. Hence, the convergence performance of a MIMO equalizer is highly dependent on the

cross-correlation of the individual channel impulse responses. In [39], Papadias and Paulraj have modified the CMA cost function for a MIMO system operating over highly correlated frequency selective channels. They introduce the following modified CMA cost function:

$$\mathrm{CF}^{\mathrm{MIMO}}_{\mathrm{CMA\text{-}PP}} = \mathrm{E}\left\{\sum_{j=1}^{N_T}[|y_j(k)|^2 - R_c^2]^2\right\} + 2\sum_{i,i'=1;i\neq i'}^{N_T}\sum_{d=d_1}^{d_2}|r_{ii'}(d)|^2, \tag{2.36}$$

where $r_{ii'}(d) = \mathrm{E}[y_i(k)\, y_{i'}^*(k-d)]$ is the cross-correlation between users $i$ and $i'$.

The second term of the new cost function penalizes the correlations between the users and pushes the cross-correlation term towards zero. The parameters $d_1$ and $d_2$ accommodate all possible delays between the $N_T$ user signals. Using this cost function the equalizer matrix can be updated as [39]:

$$\boldsymbol{F}(k+1) = \boldsymbol{F}(k) - \mu[\widehat{\boldsymbol{\Delta}}_1(k)\cdots\widehat{\boldsymbol{\Delta}}_{N_T}(k)], \tag{2.37}$$

where

$$\boldsymbol{\Delta}_j(k) = \mathrm{E}[\{|y_j(k)|^2 - R_c^2\}y_j(k)\boldsymbol{x}^*(k)] + \sum_{i'=1;i'\neq i}^{N_T}\sum_{d=d_1}^{d_2} r_{ii'}(d)\mathrm{E}[y_{i'}(k-d)\boldsymbol{x}^*(k)] \tag{2.38}$$

and $\widehat{\boldsymbol{\Delta}}_j$ is an estimate of $\boldsymbol{\Delta}_j$. The estimation can be based on instantaneous values or sample averaging. But, the estimation slows the blind equalization convergence, and hence this algorithm is suitable for MIMO systems where the receivers are very closely spaced, yielding very high cross-correlations.

In [3], Li and Liu have also used a cross-correlation penalty function to get rid of the co-channel interference. Their modified CMA cost function is:

$$\mathrm{CF}^{\mathrm{MIMO}}_{\mathrm{CMA\text{-}LL}} = \mathrm{E}\left\{\sum_{j=1}^{N_T}[|y_j(k)|^2 - R_c^2]^2\right\} - b_o\sum_{i,i'=1;i\neq i'}^{N_T}K(y_i, y_{i'}), \tag{2.39}$$

where $b_o \geq m_{4s}/(2\,m_{2s}^2 - m_{4s})$ and $K(y_i, y_{i'})$ for the case of two users can be defined as

$$\begin{aligned} K(y_1, y_2) = &\frac{1}{2} \sum_{k'=-\infty}^{-1} \mathrm{Cum}[y_1(k), y_1^*(k), y_2(k+k'), y_2^*(k+k')] \\ &+ \frac{1}{2} \sum_{k'=0}^{\infty} \mathrm{Cum}[y_1(k-k'), y_1^*(k-k'), y_2(k), y_2^*(k)], \quad \text{for all} \quad k' \leq k. \end{aligned} \tag{2.40}$$

The cumulant is defined as

$$\mathrm{Cum}(y_1, y_1^*, y_2, y_2^*) = \mathrm{E}[|y_1|^2|y_2|^2] - \mathrm{E}[|y_1|^2]\,\mathrm{E}[|y_2|^2] - |\mathrm{E}[y_1 y_2^*]|^2 \tag{2.41}$$

for complex random variables $y_j$ satisfying the condition:

$$\mathrm{E}[y_j] = \mathrm{E}[y_j^2] = 0, \quad \text{for} \quad j = 1, 2. \tag{2.42}$$

The equalizer update algorithm can be implemented for any number of users, but here we consider only two users ($i = 1, 2$). The algorithm for two users is [3]:

$$f_{ij}^n(k) = f_{ij}^{n-1}(k) - \mu\{[|y_i(n)|^2 - R_c^2]\, y_i(n) - b_o\, z_i(n)\} x_j^*(n-k), \tag{2.43}$$

where $j = 1, \ldots, N_R$, $\mu$ is a small step size, $f_{ij}^n(k)$ is the $k$-th tap weight of the $ij$-th filter after the $n$-th iteration and the $z_i(n)$'s are given by

$$\begin{aligned} z_1(n) &= \sum_{d=0}^{\infty} \{|y_2(n-d)|^2 y_1(n) - \mathrm{E}[|y_2(n-d)|^2] y_1(n) - \mathrm{E}[y_1(n) y_2^*(n-d)] y_2(n-d)\} \\ z_2(n) &= \sum_{d=0}^{\infty} \{|y_1(n-d)|^2 y_2(n) - \mathrm{E}[|y_1(n-d)|^2] y_2(n) - \mathrm{E}[y_2(n) y_1^*(n-d)] y_1(n-d)\} \end{aligned} \tag{2.44}$$

In practice $z_1(n)$ and $z_2(n)$ are replaced by their empirical averages. These averages can be easily implemented using single-pole smoothing filters, at the cost of slower equalizer convergence speed. But, as mentioned in [3], this reduction in speed often enables convergence even when the initial condition of (2.34) is not met.

In summary, the modified algorithm of (2.43) can be used until the excess kurtosis

condition (2.34) is satisfied. Then the conventional MIMO CMA algorithm without a penalty function should be used to minimize (2.27). The purpose of the new algorithm is to adjust the equalizer tap weights so that the excess kurtosis condition (2.34) is satisfied. If the initial excess kurtosis ratio satisfies the condition, then there is no need to use the modified CMA algorithm. We now consider the union of THP and blind equalizers for both SISO and MIMO systems.

# Chapter 3

# IMPLEMENTATION AND ANALYSIS OF THP-BLIND EQUALIZATION

In this chapter we derive SISO and MIMO system models for the combination of THP and blind equalization techniques. As shown in Section 2.2, the DFE is a non-linear device with a structure which can be used both for equalization and precoding. In the following sections we study these two operation modes. As an equalizer in the receiver, the feedback filter of the DFE is prone to error propagation, whereas as a precoder in the transmitter, the feedback filter does not suffer from this problem, but it increases the signal power.

After describing the system model we study the effect of THP on the statistical properties of the transmitted data signal. We then derive bounds on the higher-order moments of the THP-encoded signal.

## 3.1 DFE-BASED PRECODING OPERATION

Figures 2.2 and 2.6 show block diagrams of the DFE and the THP, with the feedback filter in the receiver and transmitter, respectively. If the $z$-transform of the channel transfer function can be represented as $H(z)$, then ideally the THP feedback filter in the precoder has the form $H(z) - 1$ as shown in Fig. 2.6. But, for most practical scenarios the channel transfer function is not known at the transmitter, and the tap weights of the precoder filter cannot be derived. Fortunately, a DFE can be used to determine practical tap weights for the precoder filter. After equalizing the channel, the tap weights of the feedback filter of the DFE are sent back to the transmitter via a reverse channel to be used for the precoder tap weights. Then, for a fixed channel

the feedback filter in the DFE is no longer needed, eliminating error propagation in the system. Only the linear feedforward part of the equalizer is retained in the receiver.

Figure 3.1 shows the training sequence mode of a DFE. In this mode, the equalizer can apply an adaptive algorithm or Wiener filter theory (if $H(z)$ is perfectly known) to determine good tap weights. At the end of the training sequence the feedback filter tap

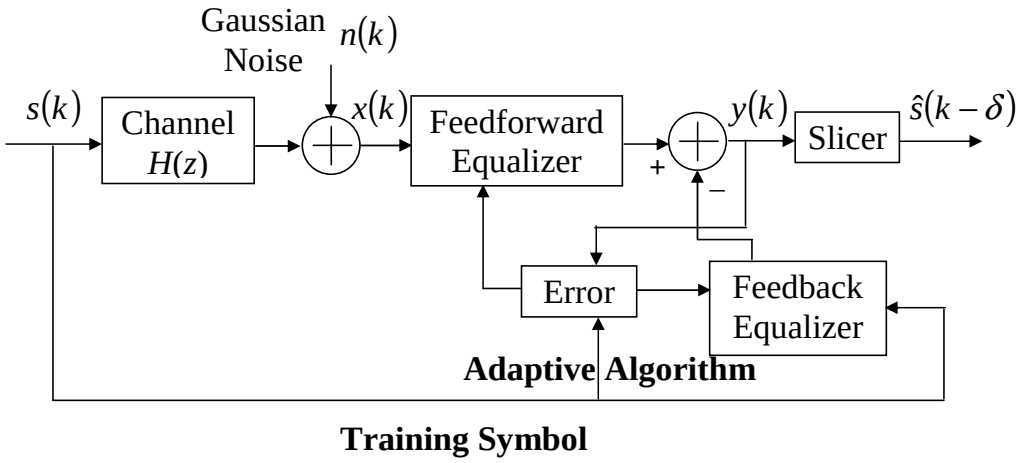


**Figure 3.1** Training sequence mode for DFE

weights are transferred to the precoder, yielding only a linear equalizer at the receiver as shown in Fig. 3.2. At this point the communication system will be in steady-state

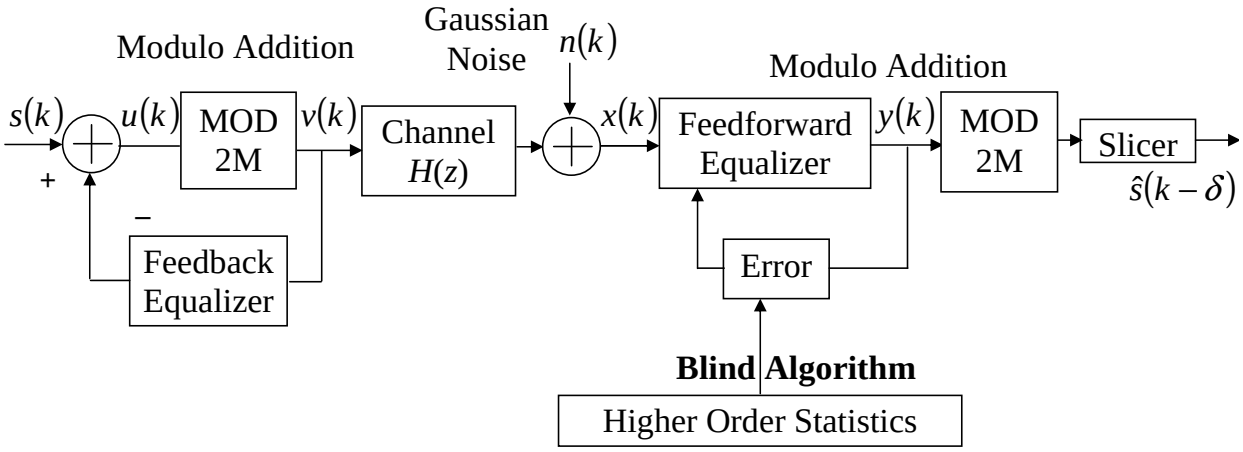


**Figure 3.2** Use of feedback filter of DFE in precoder

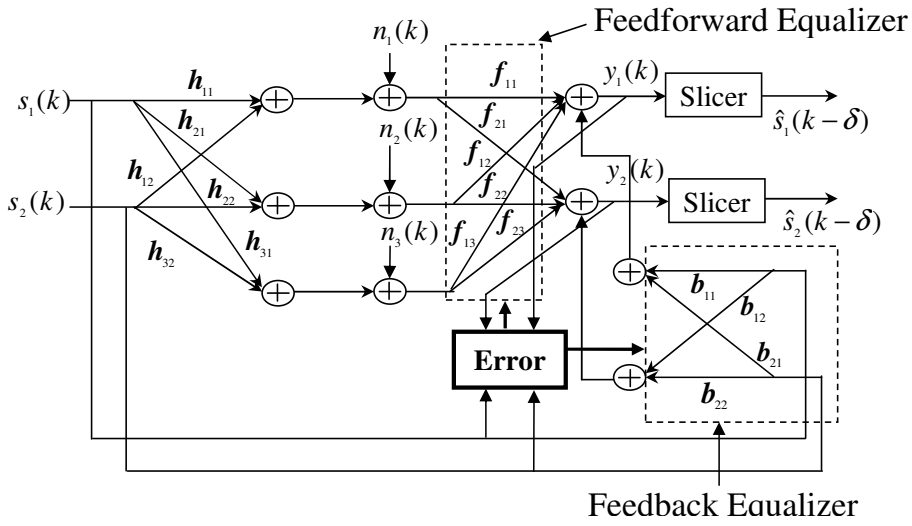


**Figure 3.3** Training sequence mode for MIMO DFE

mode. If, however, another user wants to join the broadcast or point-to-multipoint system, either the initialization process has to start again or the additional user can use an adaptive blind algorithm to deduce the tap weights of the linear equalizer while the precoder tap weights remain fixed at the values derived from the initial training sequence mode.

For a MIMO system, the CSI between each of the transmitter and receiver antennas is not known beforehand in the transmitter. So, good DFE tap weights can be determined using training. Figure 3.3 shows the training sequence mode for a $2 \times 3$ MIMO system. Similar to a SISO system, the feedback filter tap weights can be transferred to the transmitter via a reverse channel, and the steady state system model for the corresponding MIMO system is shown in Fig. 3.4.

So, the operational steps for both SISO and MIMO systems can be summarized as:

1. Train the DFE to get the optimum tap weights for the feedback filter.

2. Switch from the DFE to THP, yielding only a linear equalizer in the receiver. The feedback filter then performs the precoding operation in the transmitter.

3. Now the precoded data is passed through the channel. If another user joins the system, a blind algorithm is used to open the "eye".

*Precoder vs. DFE Feedback Tap Weights*

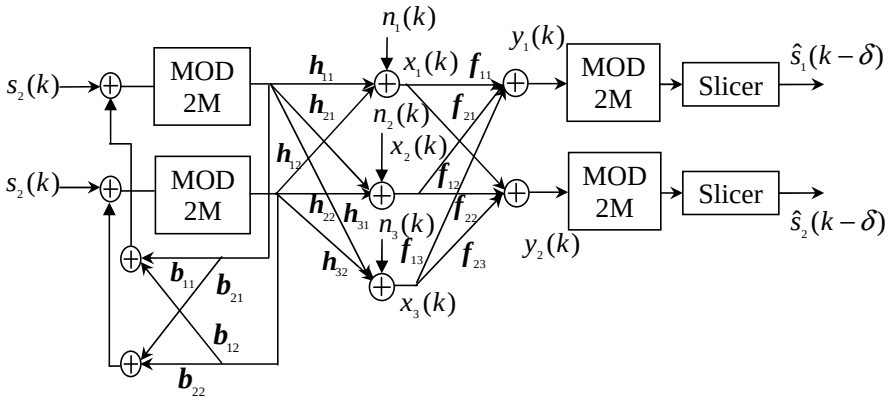


**Figure 3.4** Use of feedback filter of MIMO DFE in precoder

We now investigate the relationship of the feedback filter tap weights of the DFE to the optimal THP feedback filter tap weights introduced in Section 2.4. To do this, we consider a simple zero channel using a DFE with $N_f = 2$ and $N_b = 1$. As the channel consists of a single zero, its length is $L = 2$. The $z$-transform of the channel impulse response can be written as $H(z) = 1 + \alpha\, z^{-1}$, where $\alpha$ represents the single complex zero in the channel. Thus, the transfer function of the precoder feedback filter has the simple form $\alpha\, z^{-1}$. So, the THP filter in the transmitter is a one-tap finite impulse response (FIR) filter with a single complex tap weight $\alpha$.

Because we know the channel impulse response, using Wiener filter theory we can determine the optimum tap weights of the DFE. As we will show, in the case of a zero forcing (ZF) equalizer, the optimal tap weights of the feedback filter match the theoretical THP tap weights. But, given channel noise, the Wiener tap weights differ from the theoretical THP tap weights. Note that the use of THP removes the noise enhancement problem of the ZF equalizer.

Using vector notation, the channel impulse response of the single zero channel can be expressed as $\boldsymbol{h} = [1 \quad \alpha]$. Now, the channel convolution matrix $\boldsymbol{H}$ is a 2 by 3 matrix of the form

$$\boldsymbol{H} = \begin{bmatrix} 1 & \alpha & 0 \\ 0 & 1 & \alpha \end{bmatrix}. \tag{3.1}$$

For this channel, we find that

$$\mathrm{E}\{\boldsymbol{x}\,\boldsymbol{x}^H\} = \sigma_s^2 \begin{bmatrix} 1+|\alpha|^2 & \alpha \\ \alpha^* & 1+|\alpha|^2 \end{bmatrix} + \sigma_n^2\,\boldsymbol{I}_2$$

$$\mathrm{E}\{\boldsymbol{x}\,\boldsymbol{s}_B^H\} = \sigma_s^2 \begin{bmatrix} 1 & \alpha & 0 \\ 0 & 1 & \alpha \end{bmatrix} \begin{bmatrix} \mathbf{0}_{\delta\times 1} \\ 1 \\ \mathbf{0}_{(2-\delta)\times 1} \end{bmatrix},$$

where $(\cdot)^*$ denotes the complex conjugate. Similarly, the cross-correlation vector $\boldsymbol{p}_\delta$ has the form

$$\boldsymbol{p}_\delta = \sigma_s^2 \begin{bmatrix} \boldsymbol{H}(:,\delta) \\ 0 \end{bmatrix}. \tag{3.2}$$

For specific delay $\delta = 1$, we have

$$\mathrm{E}\{\boldsymbol{x}\,\boldsymbol{s}_B^H\} = \sigma_s^2 \begin{bmatrix} 1 & \alpha & 0 \\ 0 & 1 & \alpha \end{bmatrix} \begin{bmatrix} 0 \\ 1 \\ 0 \end{bmatrix} = \sigma_s^2 \begin{bmatrix} \alpha \\ 1 \end{bmatrix}.$$

From (2.7) and (2.11) the corresponding autocorrelation matrix and cross-correlation vector are

$$\boldsymbol{R}_{\delta=1} = \begin{bmatrix} \sigma_s^2(1+|\alpha|^2)+\sigma_n^2 & \sigma_s^2\,\alpha & -\sigma_s^2\,\alpha \\ \sigma_s^2\,\alpha^* & \sigma_s^2(1+|\alpha|^2)+\sigma_n^2 & -\sigma_s^2 \\ -\sigma_s^2\,\alpha^* & -\sigma_s^2 & \sigma_s^2 \end{bmatrix} \tag{3.3}$$

$$\boldsymbol{p}_{\delta=1} = \sigma_s^2\,[1 \quad 0 \quad 0]^H. \tag{3.4}$$

For the case of $\sigma_n^2 = 0$, corresponding to the ZF solution, the optimum tap weights

have the form

$$\boldsymbol{w}_{\delta=1} = \begin{bmatrix} 1 & 0 & \alpha \\ 0 & \frac{1}{|\alpha|^2} & \frac{1}{|\alpha|^2} \\ \alpha^* & \frac{1}{|\alpha|^2} & \frac{1+|\alpha|^2+|\alpha|^4}{|\alpha|^2} \end{bmatrix} \begin{bmatrix} 1 \\ 0 \\ 0 \end{bmatrix} = \begin{bmatrix} 1 \\ 0 \\ \alpha \end{bmatrix} \tag{3.5}$$

and

$$\boldsymbol{f}_{\delta=1} = [1 \quad 0]^H \qquad \boldsymbol{b}_{\delta=1} = \alpha. \tag{3.6}$$

Similarly, for $\delta = 2$ we find

$$\mathrm{E}\{\boldsymbol{x}\, \boldsymbol{s}_B^H\} = \sigma_s^2 \begin{bmatrix} 0 \\ \\ \alpha \end{bmatrix}$$

$$\boldsymbol{R}_{\delta=2} = \begin{bmatrix} \sigma_s^2(1+|\alpha|^2)+\sigma_n^2 & \sigma_s^2\,\alpha & 0 \\ \sigma_s^2\,\alpha^* & \sigma_s^2(1+|\alpha|^2)+\sigma_n^2 & -\sigma_s^2\,\alpha \\ 0 & -\sigma_s^2\,\alpha^* & \sigma_s^2 \end{bmatrix}$$

$$\boldsymbol{p}_{\delta=2} = [\sigma_s^2\,\alpha^* \quad \sigma_s^2 \quad 0]^H.$$

Again for $\sigma_n^2 = 0$, the ZF tap weights are

$$\boldsymbol{w}_{\delta=2} = [0 \quad 1 \quad \alpha^*]^H \tag{3.7}$$

and

$$\boldsymbol{f}_{\delta=2} = [0 \quad 1]^H \qquad \boldsymbol{b}_{\delta=2} = \alpha^*. \tag{3.8}$$

Now we can use (2.6) to find the optimum delay, producing the minimum mean-squared error (MMSE). But, for a single real zero channel with a 10 dB SNR it is shown in Fig. 3.5 that the MMSE is attainable for a delay of 2. Hence, by choosing this optimum delay, the optimal tap weights of the feedforward and feedback filters are shown in (3.8).

It is clear that the feedback filter tap weight exactly matches the desired precoder

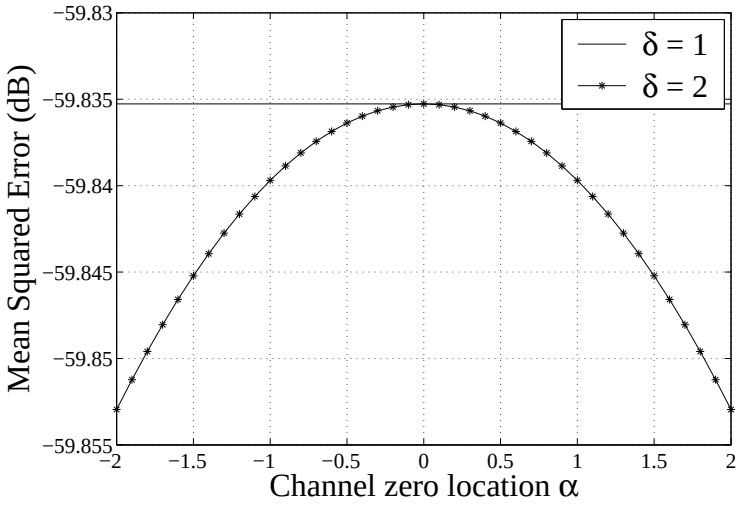


**Figure 3.5** MMSE for different values for zero of the channel and propagation delay

tap weight for the ZF solution. In practice, Wiener filter theory cannot be applied as the channel conditions will be changing and unknown. Rather, an adaptive algorithm, such as the LMS algorithm, is applied in training sequence mode to find the tap weights. Therefore, the success of this process of finding the precoder tap weights largely depends on the tracking ability of the particular adaptive algorithm. If it can be shown that the tap weights found from an adaptive algorithm closely approximate the Wiener filter tap weights, then we can conclude that the adaptive process works well for finding the precoder tap weights.

To do this, let us consider a complex baseband channel from [2]. Its impulse response is shown in Fig. 3.6; it consists of both precursors and postcursors. The channel output is also corrupted by additive white Gaussian noise with 0 dB SNR. We use a symbol-spaced DFE with 3 feedforward taps and 3 feedback taps to remove the distortions introduced by the channel and noise.

Assuming full knowledge of the CSI, we can use Wiener filter theory to derive the optimum tap weights of the DFE. If the CSI is unknown, we can send a training sequence to adapt the equalizer. In this mode, the feedforward taps are initialized with zero, except for the rightmost tap which is set to 1. All the feedback taps are initialized to zero. We use the LMS algorithm with a step size of 0.01 to adapt the DFE. Figure 3.7 shows the gradual reduction of the MSE between the equalizer outputs and the training symbols. By 250 iterations, the error settles down, and we can stop

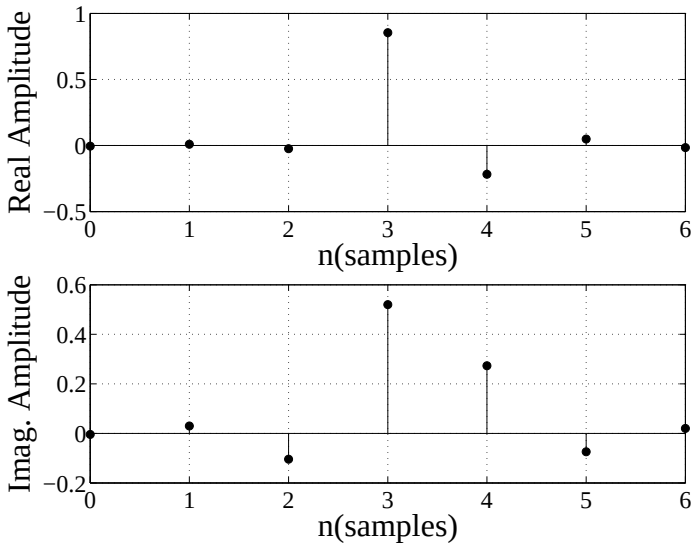


**Figure 3.6** Channel impulse response from [2]

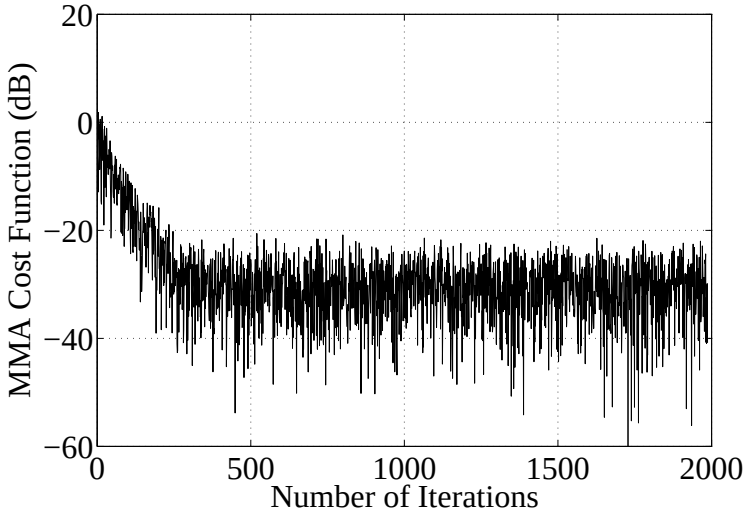


**Figure 3.7** MSE during training sequence

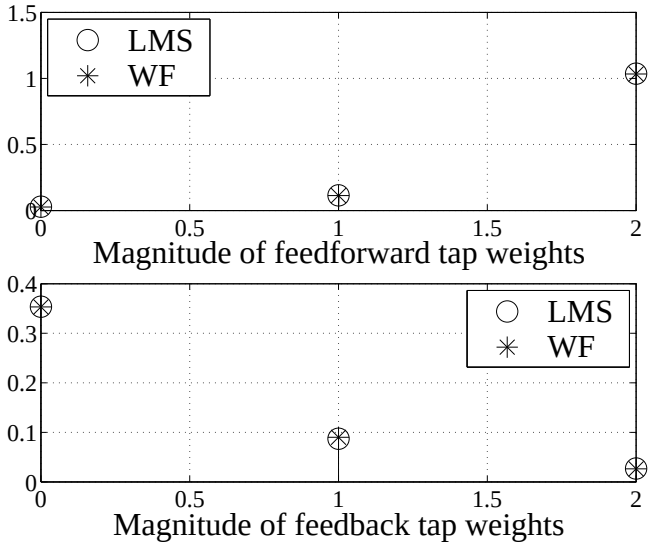


**Figure 3.8** Comparison of DFE tap weight magnitudes

sending training data. The steady state tap weights of the DFE are compared with the Wiener filter DFE tap weights in Fig. 3.8. We see that for this particular channel the LMS algorithm tap weights converge to the optimal tap weights. Hence, as THP tap weights we can use the feedback tap weights found from training the DFE.

Note that the purpose of the pre-equalization filter in the transmitter is to subtract out the i.s.i. introduced by the postcursors of the channels [48]. Ideally, the tap weights of these two filters should be equal to the channel postcursors. Comparing the respective magnitudes in Fig. 3.9, this specification has also been achieved for this channel.

## 3.2 THP: KURTOSIS BOUND

In our research we have found that a helpful by-product of THP is that it aids blind equalization by controlling the transmitted signal statistics. Recall that, using the modulo operation, the Tomlinson-Harashima precoder (THP) bounds the transmitted signal power. Thus, the modulo adder, as shown in Fig. 2.6, can have a great impact on the performance of blind equalization. In blind equalization the received observations are aligned to some fixed value of the source statistics. Most often the fixed value depends on the transmitted signal kurtosis (2.28) [8].

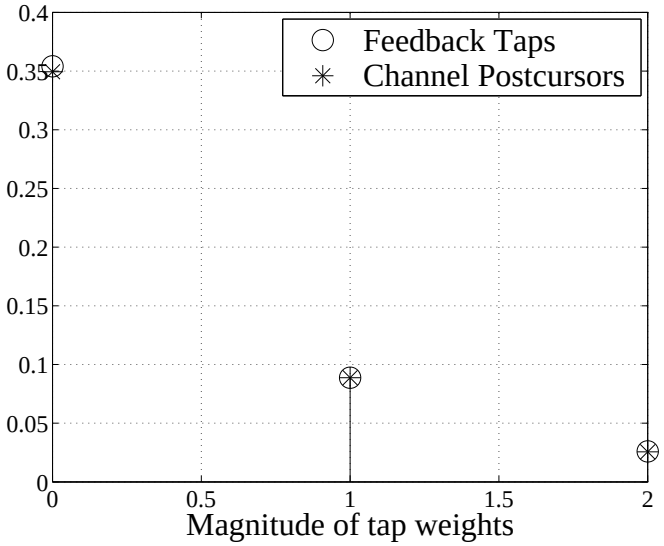


**Figure 3.9** Comparison of feedback filter tap weights with channel postcursors

### 3.2.1 Effect of THP on Blind Equalization

In [9], [10] it has been shown that the source data correlation plays a significant role in the convergence of blind adaptive equalizers. An $M$-ary ASK signal can be categorized according to its kurtosis [10]. A Gaussian signal with $\kappa_s = 3$ is known as meso-kurtic, and it causes the ill-convergence of Bussgang-type blind algorithms. The signal is known as sub-Gaussian for $\kappa_s < 3$ and super-Gaussian for $\kappa_s > 3$. Bussgang-type blind algorithms only fare well for sub-Gaussian type source distributions [8], [9]. (Note that for complex signal distributions the threshold value is $\kappa_s = 2$, corresponding to a complex Gaussian signal).

Ideally the kurtosis needs to be bounded below three for good convergence of Bussgang-type blind algorithms. It can be shown both mathematically and using Monte Carlo simulations that the THP operation bounds the kurtosis below the Gaussian mark.[1]

As an example, let us consider the single-zero channel whose transfer function can be represented as $H(z) = 1 + \alpha\, z^{-1}$, where $\alpha$ represents the zero in the channel. The THP model for a single-zero channel is represented in Fig. 3.10. For an $M$-ary ASK

[1] Note that, even for sub-Gaussian signals, certain combinations of equalizer structures and Bussgang cost functions (e.g., a finite length CMA symbol-spaced equalizer) can yield incorrect steady-state solutions, where the i.s.i. has not been properly mitigated [8]. Although these incorrect solutions are theoretically interesting, in practical systems we have found that misconvergence occurs very rarely and can be easily overcome for real world channels by simply retraining the blind equalizer.

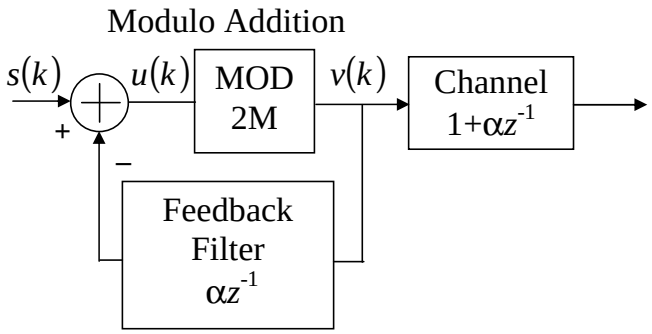


**Figure 3.10** THP model for single-zero channel

signal taking values from set $\{\pm 1, \pm 3, \cdots, \pm(M-1)\}$, with $M$ even, the modulo adder operates in the linear region for $|u(k)| \leq |M|$, where $u(k)$ is the input to the modulo operator. Whenever $|u(k)| > |M|$ the modulo adder wraps the signal to force it to lie in the $[-M,+M]$ region. When the input $s(k)$ is at its positive maximum of $(M-1)$ and $v(k)$ reaches its maximum negative value of $-M$, the modulo input $u(k)$ can cross the maximum value of $M$, depending on the value of $\alpha$. So the modulo adder performs the nonlinear operation on the modulo when

$$\begin{aligned}(M-1) + \alpha M &> M \\ \Rightarrow \alpha M &> 1 \\ \Rightarrow \alpha &> \frac{1}{M}.\end{aligned} \tag{3.9}$$

Similarly, it can be shown that for

$$\alpha < -\frac{1}{M} \tag{3.10}$$

the modulo adder performs the nonlinear operation. For a $n$-tap all zero channel with zeros denoted by $\alpha(i), i = 1, 2, \ldots n$, the nonlinear region can be expressed as:

$$\left| \sum_{i=1}^{n-1} \alpha(i) \right| > \frac{1}{M}. \tag{3.11}$$

Equations (3.9) and (3.10) give the value $\alpha$ for which the modulo adder starts to

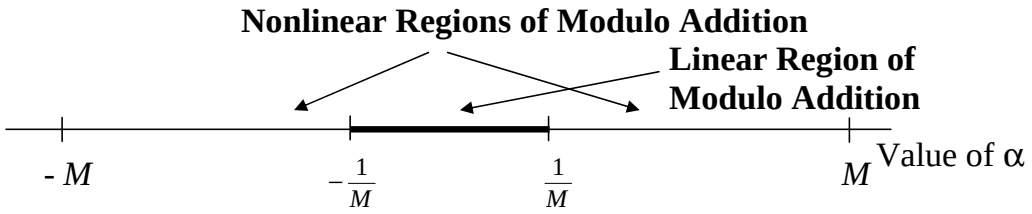


**Figure 3.11** Linear and nonlinear regions of the THP

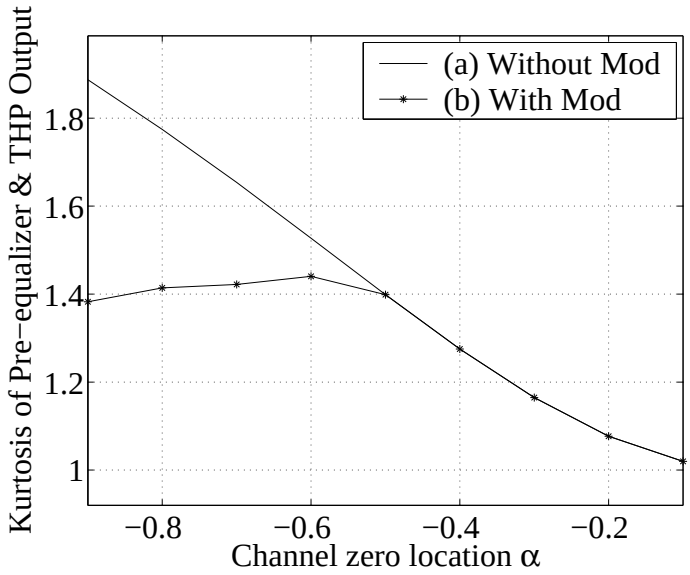


**Figure 3.12** Prefiltered signal kurtosis for 4-QAM over single-zero channel (a) without and (b) with modulo operator

perform the nonlinear operation, and it directly depends on the signal constellation size. As the constellation size increases, the nonlinearity of the modulo adder increases as shown in Fig. 3.11. For very large $M$, the linear region of the modulo adder becomes very small, and hence the kurtosis becomes constant even for a small channel zero magnitude. This will be shown in the next section. Using Monte Carlo simulations, this kurtosis bounding effect of THP can be compared with a pre-equalizer without the modulo operation. Figures 3.12 and 3.13 show the bounding effect for 4-QAM and 16-QAM as a function of $\alpha$. These figures are generated with 10,000 data points averaged over 10 trials.

For a MIMO system, let us consider a $2 \times 2$ MIMO system where each individual channel transfer function is assumed to have a single zero. We also assume that each

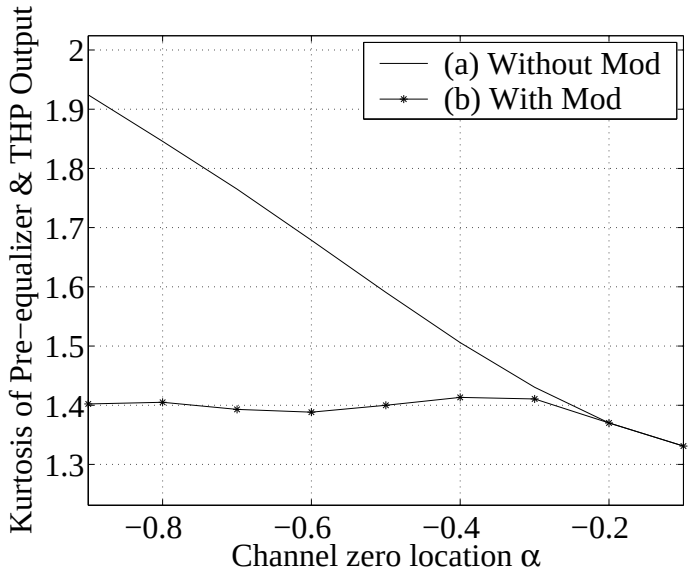


**Figure 3.13** Prefiltered signal kurtosis for 16-QAM over single-zero channel (a) without and (b) with modulo operator

zero of this $2 \times 2$ MIMO system is different. The corresponding $2 \times 2$ THP for this channel model is shown in Fig 3.14. The transmitted signals are chosen from the $M$-ary ASK signal set $\{\pm 1, \pm 3, \cdots, \pm(M-1)\}$, with $M$ even. Both the modulo adders operate in the linear region if $|u_1(k)| \leq |M|$ and $|u_2(k)| \leq |M|$. The wrapping around by the modulo adders starts when $|u_1(k)| > |M|$ or $|u_2(k)| > |M|$. So, considering $u_1(k)$, the nonlinear operation starts when

$$\begin{aligned} (M-1) &+ \alpha_{11} M + \alpha_{12} M > M \\ &\Rightarrow (\alpha_{11} + \alpha_{12}) M > 1 \\ &\Rightarrow \alpha_{11} + \alpha_{12} > \frac{1}{M}. \end{aligned} \tag{3.12}$$

Similarly, it can be shown that for

$$\alpha_{11} + \alpha_{12} < -\frac{1}{M} \tag{3.13}$$

the modulo adder for the $u_1(k)$ stream performs the nonlinear operation in the reverse direction.

Therefore, it can be inferred that the linear region of operation of the modulo adder

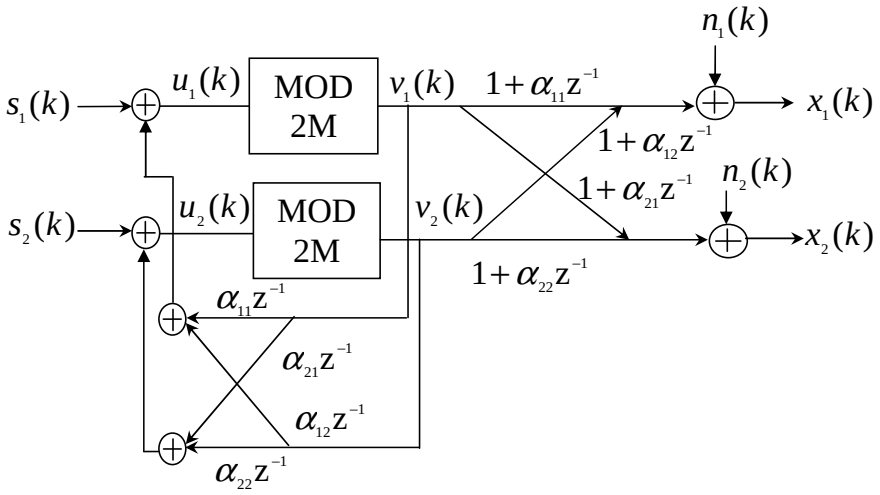


**Figure 3.14** $2 \times 2$ MIMO THP system

for a MIMO system is smaller than that of a SISO system, and it decreases as the number of transmitters increases. This bounding effect for MIMO systems is compared with a pre-equalizer without a modulo operation using Monte Carlo simulations in Figs. 3.15 and 3.16 for 4-QAM and 16-QAM.

### 3.2.2 Analytical Bound on the Kurtosis for THP-Generated Signals

In [48], Mazo and Salz derive a theoretical bound for the second moment of a THP system. This bound for an $M$-ary ASK signal is

$$\frac{M^2-1}{3} \leq \mathrm{E}\{v^2(k)\} \leq \frac{M^2-1}{3}+1, \quad k=1,2,\ldots \tag{3.14}$$

where $v(k)$ is the precoder output shown in Fig. 2.6. We now extend their analysis to bound the fourth moment $\mathrm{E}\{v^4(k)\}$ and the kurtosis $\kappa_v$.

*Kurtosis Bound for THP-Encoded ASK Symbols*

First consider an $M$-ary ASK source with $a(k)$ chosen from equi-spaced symbol levels $\{\pm 1, \pm 3, \ldots, \pm(M-1)\}$, with $M$ even. We assume that each constellation point is equi-probable with probability $1/M$. Due to symmetry about zero of the source

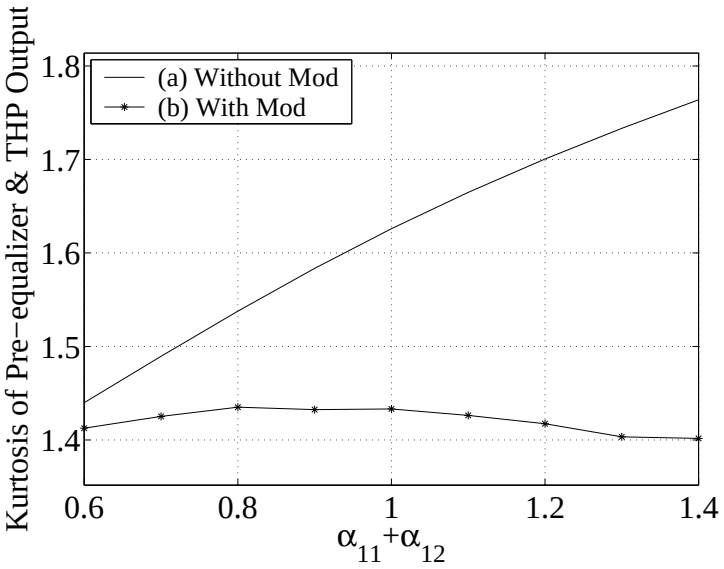


**Figure 3.15** Prefiltered signal kurtosis for 4-QAM in $u_1(k)$ stream over single-zero MIMO channel (a) without and (b) with modulo operator between $u_1(k)$ and $v_1(k)$

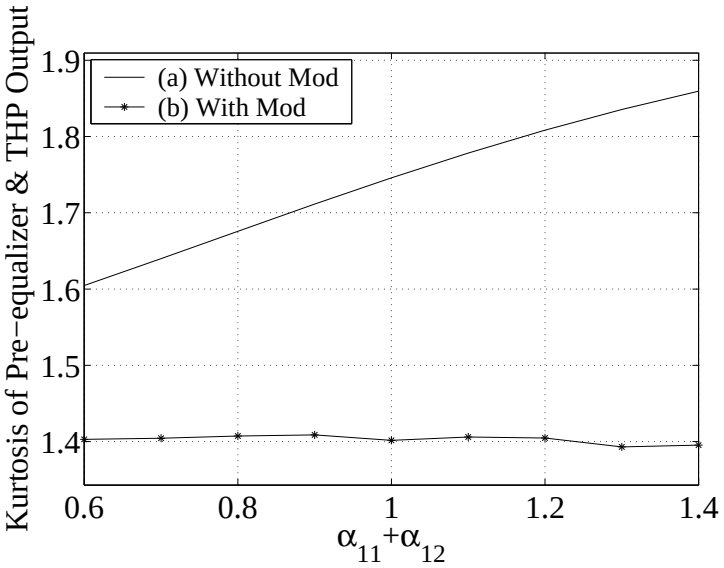


**Figure 3.16** Prefiltered signal kurtosis for 16-QAM in $u_1(k)$ stream over single-zero MIMO channel (a) without and (b) with modulo operator between $u_1(k)$ and $v_1(k)$

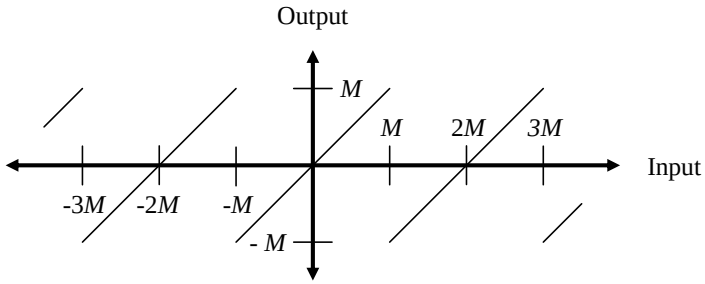


**Figure 3.17** Sawtooth input-output function of the modulo adder

signal constellation, the fourth moment of the $M$-ary ASK signal can be expressed as:

$$\mathrm{E}\{a^4(k)\} = \frac{1}{L}\sum_{i=1}^{L}(2\,i-1)^4 = \frac{48\,L^4 - 40\,L^2 + 7}{15} = \frac{3\,M^4 - 10\,M^2 + 7}{15},$$

where $L = M/2$.

The modulo adder performs the "sawtooth" function shown in Fig. 3.17 and does not affect $u(k)$ until it crosses a certain limit. Whenever it crosses the limit, the adder wraps the result to make sure that the sum is within $[-M, +M]$.

In the THP system of Fig. 2.6, the output of the modulo adder can be expressed as [48]:

$$v(k) = \begin{cases} g\left[s(k) - \sum_{i=1}^{N}\beta(i)\,v(k-i)\right], & k = 1,\, 2,\, \ldots \\ 0, & k = 0,\, \text{-}1,\, \text{-}2,\, \ldots \end{cases} \tag{3.15}$$

where function $g(u)$ executes the modulo addition and the $\beta(i)$'s are the feedback filter tap weights within the THP. We can rewrite the THP output as

$$v(k) = g[s(k) + \theta(k)], \tag{3.16}$$

where $\theta(k)$ is a symmetric random variable, independent of $s(k)$. The fourth moment of $v(k)$ is then

$$\mathrm{E}\{v^4(k)\} = \frac{1}{M}\sum_{i=1}^{M}\int g^4[m_i + \theta]\, f_\Theta(\theta)\, d\theta, \tag{3.17}$$

where $m_i$ takes the $M$ different values of $s(k) \in \{\pm 1, \pm 3, \ldots, \pm(M-1)\}$ with equal

probability. As shown in [48], the probability density function of $\theta$ can be approximated with arbitrary accuracy by a finite sum of delta functions

$$f_\Theta(\theta) \cong \sum_i d_i \, \delta \, (\theta - \xi_i). \tag{3.18}$$

Note that the contribution of each delta function to $\mathrm{E}\{v^4(k)\}$ is additive.

Now consider the THP output $v(k)$ for the specific component value $\xi_o$. For $|\xi_o| \leq 1$ the output is a random variable taking the $M$ values

$$-(M-1)+\xi_o, -(M-1)+\xi_o+2, \ldots, (M-1)+\xi_o$$

with equal probability. Likewise, for $\xi_o > 0$ the output for the shifted component $\xi_o + 2$ is a random variable taking the $M$ values

$$-(M-1)+\xi_o+2, -(M-1)+\xi_o+4, \ldots, g[(M-1)+\xi_o+2] = -(M-1)+\xi_o$$

with equal probability. Thus, the outputs $g[s(k)+\xi_o]$ and $g[s(k)+\xi_o+2]$ have the same distribution. In general, $g[s(k)+\xi_o+2n]$, for integer $n$, has the same distribution for $|\xi_o| < 1$. Therefore, we only need to examine individual terms $d_i \, \delta \, (\theta - \xi_i)$ in (3.18) over the range $|\xi_o| \leq 1$.

Focussing on a pair of values $\pm K$ which $s(k)$ can take from $\{\pm 1, \pm 3, \ldots, \pm(M-1)\}$, from (3.17) we see that this pair produces a contribution to $\mathrm{E}\{v^4(k)\}$ proportional to

$$(K+\xi)^4 + (K-\xi)^4 = 2\,K^4 + 12\,K^2\xi^2 + 2\,\xi^4. \tag{3.19}$$

Over the range $|\xi| \leq 1$, value (3.19) is minimized for $\xi = 0$ and maximized for $\xi = \pm 1$, regardless of which $K$ is selected.

Then, the minimum value of $\mathrm{E}\{v^4(k)\}$ is obtained by taking $\xi = 0$, $d = 1$ in (3.18), yielding

$$\mathrm{E}\{v^4(k)\} \geq \mathrm{E}\{s^4(k)\} = \frac{3\,M^4 - 10\,M^2 + 7}{15}. \tag{3.20}$$

**Table 3.1** Kurtosis for $M$-ary ASK

| $M$-ary ASK | Input Symbol Kurtosis | Calculated Lower Bound | Calculated Upper Bound | Simulated THP Output Kurtosis |
|---|---|---|---|---|
| 4 | 1 | 1.1389 | 2.8800 | 1.6523 |
| 16 | 1.6486 | 1.7492 | 1.8613 | 1.7806 |
| 64 | 1.7571 | 1.7968 | 1.8038 | 1.8003 |

Similarly, an upper bound can be formed by taking $\xi = 1$, $d = 1$ in (3.18), yielding

$$\mathrm{E}\{v^4(k)\} \le \mathrm{E}\{[s(k)+1]^4\} = 1 + 4\,\mathrm{E}\{s(k)\} + 6\,\mathrm{E}\{s^2(k)\} + 4\,\mathrm{E}\{s^3(k)\} + \mathrm{E}\{s^4(k)\}.$$

As the odd-ordered moments for a symmetric random variable are zero, the expectation reduces to

$$\begin{aligned}\mathrm{E}\{v^4(k)\} &\le 1 + 6\,\mathrm{E}\{s^2(k)\} + \mathrm{E}\{s^4(k)\} \\ &= 1 + 6\,\frac{M^2-1}{3} + \frac{3\,M^4 - 10\,M^2 + 7}{15} = \frac{3\,M^4 + 20\,M^2 - 8}{15}. \end{aligned} \tag{3.21}$$

Finally, the fourth moment is bounded by

$$\frac{3\,M^4 - 10\,M^2 + 7}{15} \le \mathrm{E}\{v^4(k)\} \le \frac{3\,M^4 + 20\,M^2 - 8}{15}. \tag{3.22}$$

Using (3.14) and (3.22), the kurtosis of a transmitted $M$-ary ASK signal after a THP system is bounded by:

$$\frac{9\,M^4 - 30\,M^2 + 21}{5\,M^4 + 20\,M^2 + 20} \le \kappa_v \le \frac{9\,M^4 + 60\,M^2 - 24}{5\,M^4 - 10\,M^2 + 5}. \tag{3.23}$$

Table 3.1 shows the kurtosis of the input symbols, the calculated lower and upper bounds of the kurtosis and the simulated THP output kurtosis for a single-zero channel with $\alpha = -0.8$ for a variety of $M$-ary ASK signals. The simulated values lie within the bounds. By the Central Limit Theorem, pre-filtering a signal has an averaging effect, potentially making the output more Gaussian. We have shown that THP actually bounds the output kurtosis away from 3. Regardless of the THP prefilter characteristics, from (3.22) we see that asymptotically for larger constellations ($M \to \infty$) the

lower and upper bounds converge together to the constant 1.8, ensuring the THP output is sub-Gaussian. This constant 1.8 is also the kurtosis for an uniformly distributed signal. This near uniform distribution for the THP output sequence was previously mentioned in [48] [49].

*Kurtosis Bound for THP-Encoded QAM Symbols*

In a THP system an $M$-ary QAM signal source can be treated as two uncoupled $M$-ary ASK sources [48]. Therefore, the theoretical bound on the second moment for the $M$-level THP output can be expressed as

$$2\,\frac{M^2-1}{3} \le \mathrm{E}\{|v(k)|^2\} \le 2\,\frac{M^2-1}{3} + 1, \quad k = 1, 2, \ldots \tag{3.24}$$

But the bound on the fourth moment is not as straightforward. The fourth moment of the input symbol $s(k) = a(k) + j\,b(k)$ can be evaluated as:

$$\begin{aligned}\mathrm{E}\{|s(k)|^4\} &= \mathrm{E}\{[|s(k)|^2]^2\} = \mathrm{E}\{a^4(k)\} + 2\,\mathrm{E}\{a^2(k)\}\,\mathrm{E}\{b^2(k)\} + \mathrm{E}\{b^4(k)\} \\ &= \frac{28\,M^4 - 80\,M^2 + 52}{45}.\end{aligned} \tag{3.25}$$

Using the same analogy from $M$-ary ASK, the lower bound on the fourth moment of the THP output signal is:

$$\mathrm{E}\{|v(k)|^4\} \ge \mathrm{E}\{|s(k)|^4\} = \frac{28\,M^4 - 80\,M^2 + 52}{45}. \tag{3.26}$$

The upper bound can be evaluated by expanding the equation:

$$\mathrm{E}\{|v(k)|^4\} \le \mathrm{E}\{|s(k)+1|^4\} = \mathrm{E}\left[\{[1+a(k)]^2 + b^2(k)\}^2\right].$$

As the odd order moments for symmetric symbol distributions vanish to zero, we have

$$\begin{aligned}\mathrm{E}\{|v(k)|^4\} &\le \mathrm{E}\{|s(k)|^4\} + 6\,\mathrm{E}\{a^2(k)\} + 2\,\mathrm{E}\{b^2(k)\} + 1 \\ &= \frac{28\,M^4 + 40\,M^2 - 23}{45}.\end{aligned} \tag{3.27}$$

**Table 3.2** Kurtosis for $M$-ary QAM

| $M$-ary ASK | Input Symbol Kurtosis | Calculated Lower Bound | Calculated Upper Bound | Simulated THP Output Kurtosis |
|---|---|---|---|---|
| 4 | 1 | 0.9167 | 1.7300 | 1.3203 |
| 16 | 1.3251 | 1.3630 | 1.4189 | 1.3886 |
| 64 | 1.3673 | 1.3977 | 1.4012 | 1.4006 |

Hence, the kurtosis for an $M$-ary QAM signal after THP-encoding is bounded by:

$$\frac{7\,M^4 - 20\,M^2 + 13}{5\,M^4 + 20\,M^2 + 20} \leq \kappa_v \leq \frac{28\,M^4 + 40\,M^2 - 23}{20\,M^4 - 40\,M^2 + 20}. \tag{3.28}$$

Table 3.2 shows the calculated lower and upper bounds of the kurtosis and the simulated THP output kurtosis for a single-zero channel with $\alpha = -0.8$ for a variety of $M$-ary QAM signals. It clearly shows that the kurtosis is again bounded away from 2 for $M$-ary QAM by the THP system, yielding a sub-Gaussian transmitted signal. Similar to the ASK case, as the constellation size increases the lower and upper bounds asymptotically converge to the constant 1.4, which is the kurtosis for a 2-dimensional uniformly distributed signal.

*Kurtosis Bounds for THP-Encoded MIMO Symbols*

The methodology used to formulate bounds on the THP-encoded SISO system can be easily extended to MIMO systems. We assume that all the symbols are chosen with equal probability from an $M$-ary ASK/QAM source with equi-spaced symbol levels. The THP output corresponding to $u_1(k)$ in Fig. 3.14 can be expressed as

$$v_1(k) = \begin{cases} g\left[s_1(k) - \sum_{i=1}^{N}\{\beta_1(i)\,v_1(k-i) + \beta_2(i)\,v_2(k-i)\}\right], & k = 1,\, 2,\, \ldots \\ 0, & k = 0,\, \text{-}1,\, \text{-}2,\, \ldots \end{cases} \tag{3.29}$$

where $g(u)$ represents the modulo addition and the $\beta_j(i)$'s are the feedback filter tap weights within the THP. This output can be rearranged as

$$v_1(k) = g[s_1(k) + \theta_1(k) + \theta_2(k)] \tag{3.30}$$

where $\theta_1(k)$ and $\theta_2(k)$ are symmetric random variables, independent of $\boldsymbol{s}(k)$, but dependent on each other. The fourth moment of the THP output $v_1(k)$ is then

$$\mathrm{E}\{v_1^4(k)\} = \frac{1}{M}\sum_{i=1}^{M}\int\int g^4[m_i + \theta_1 + \theta_2]\, f_\Theta(\theta_1, \theta_2)\, d\theta_1\, d\theta_2. \tag{3.31}$$

The joint probability density function of $\theta_1$ and $\theta_2$ can be approximated as a finite sum of 2-dimensional delta functions

$$f_\Theta(\theta_1, \theta_2) \cong \sum_{i,j} d_{ij}\, \delta(\theta_1 - \xi_i,\, \theta_2 - \xi_j). \tag{3.32}$$

For a specific pair $(\xi_{io}, \xi_{jo})$, such that $\xi_{io} + \xi_{jo} < 1$, the THP output $v_1(k)$ is a random variable taking $M$ values with equal probability. These $M$ values only differ from each other by $2n$, for integer $n$. In fact, the modulo output $g[s_1(k) + \xi_{io} + \xi_{jo} + 2n]$ has the same distribution for $\xi_{io} + \xi_{jo} < 1$. This implies that we can reapply the SISO methodology to the MIMO case. Therefore, the kurtosis bounds for each THP-encoded output of a MIMO system (e.g. $v_1(k)$ and $v_2(k)$) are the same as those for SISO systems.

### 3.2.3 Simulated Constellations of THP-Generated Signals

The bounding effect of the THP on the signal kurtosis can be better understood using simulated signal constellations. First, we consider a 4-QAM data source transmitted over a a single complex zero channel ($\alpha = -0.9\, e^{-j\frac{\pi}{4}}$). The simulated data source and

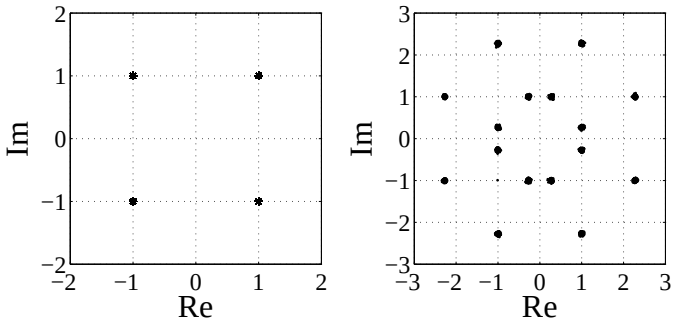


**Figure 3.18** 4-QAM (a) data source and (b) channel output constellations

channel output constellations for this channel are shown in Fig. 3.18. The channel

expands and rotates the data passing through it. The THP pre-equalizer with proper tap weights can remove the channel distortion. Using (3.8), the optimum feedback tap for this particular channel is the complex conjugate of the zero of the channel. Figure 3.19 shows the effect of the THP feedback filter without and with the modulo addition. Without the modulo addition, we see the power expansion and the Gaussian-

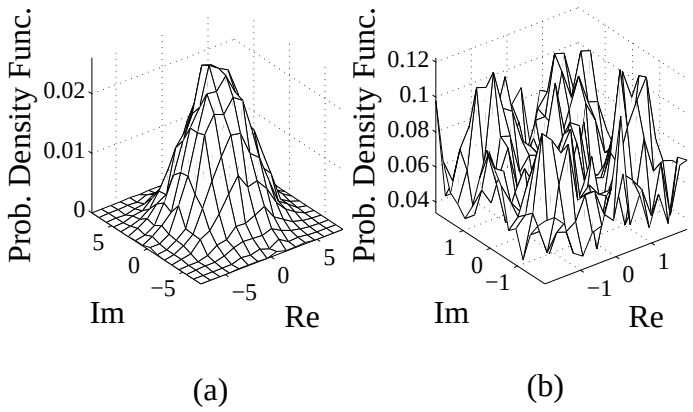


**Figure 3.19** Histograms of prefilter outputs for 4-QAM (a) without and (b) with modulo addition

like distribution of the prefilter outputs. Whereas, with the modulo addition, the THP outputs are more uniformly distributed over the square region $[-M, +M]$ without significant power expansion. With the modulo addition, the THP outputs are much better conditioned for blind equalization due to their reduced kurtosis. THP bounds the constellation even for a larger number of source symbols. The analogous histograms of the THP output constellations for 64-QAM are shown in Fig. 3.20.

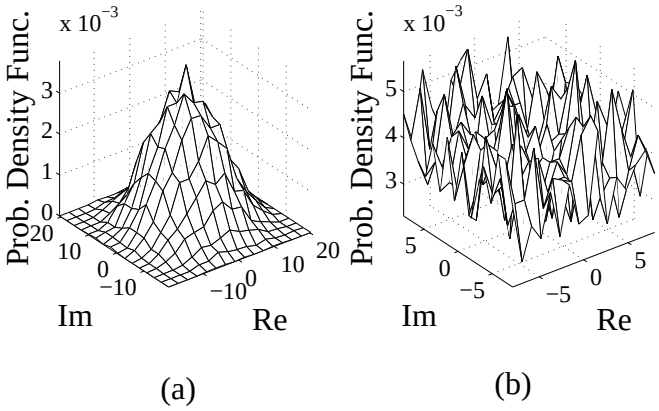


**Figure 3.20** Histograms of prefilter outputs for 64-QAM (a) without and (b) with modulo addition

# Chapter 4

# SIMULATION RESULTS

In this chapter we use Monte Carlo simulations to verify the feasibility of a full blind equalization system with THP both for SISO and MIMO systems. We also consider adding a new user to a SISO system with THP.

## 4.1 SIMULATIONS FOR SISO SYSTEMS

Using Monte Carlo simulations, we now consider the feasibility of a full blind equalization system with THP, operating in the mode outlined in Section 3.1. The 4-QAM symbols pass through a near baseband VDSL channel with additive white Gaussian noise. The SNR is set to 10 dB. We send the symbols at a rate of 12.96 Mbaud over 300 m of a 0.4 mm (26 Gauge) distribution cable with frequency and impulse responses shown in Figs. 4.1 and 4.2. Combining the effects of square-root raised-cosine pulse shaping (30% excess bandwidth) and modulation with the cable channel, the composite near baseband VDSL channel has the net frequency response shown in Fig. 4.3.

For our proposed THP-blind equalization system, first we determine the optimum tap weights for the precoder. To do this, we use an adaptive DFE with a 21-tap feedforward filter and a 15-tap feedback filter. The feedforward filter is $T/3$ fractionally-spaced and the feedback filter is symbol-spaced. The LMS algorithm is used with the aid of a training sequence. The feedback and feedforward taps are initialized to zero, except for the last tap of the feedforward filter, which is set to 1. We use a relatively large step size of 0.01. After sending 40,000 symbols (3 msec) of data the DFE opens the "eye" successfully. We stop the training mode at this point and pass the feedback filter tap weights to the transmitter via a reverse channel to be used as the precoder

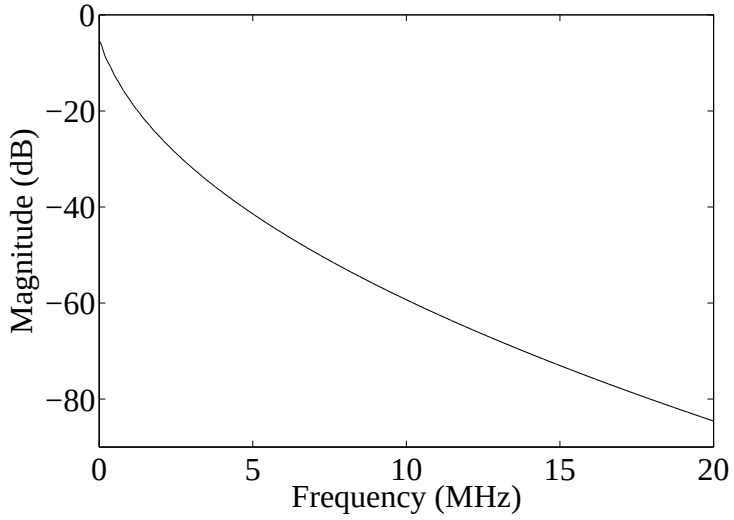


**Figure 4.1** Magnitude frequency response of 300 m of 0.4 mm distribution cable

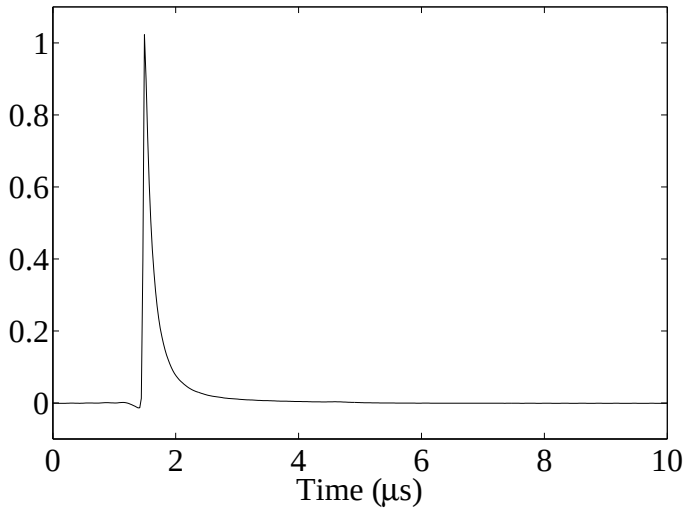


**Figure 4.2** Impulse response of 300 m of 0.4 mm distribution cable

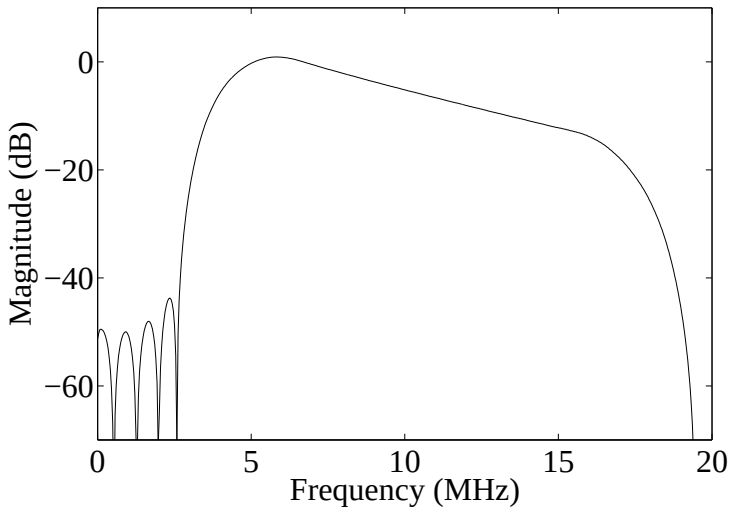


**Figure 4.3** Magnitude frequency response of composite VDSL channel

tap weights.

Now, we have the desired system model with THP in the transmitter and a linear equalizer at the receiver. At this point, a receiver wants to connect with the THP transmitter without using any training data. So we use a blind algorithm for adapting the receiver. In particular, we use the MMA algorithm to adapt the $T/3$-spaced linear equalizer. The equalizer tap weights are initialized to zero, except for the center tap which is set to 1. The step size is set to 0.05. Again, to invert the modulo addition of the THP transmitter, we need the same modulo operator after the equalizer in the receiver to restore the received data to the required dimensions. The gradual reduction of the MSE using the MMA cost function (2.20) for the whole system is shown in Fig. 4.4.

During the bind equalization mode, we have also calculated the residual error using the formula

$$e_{\text{res}} = \|\boldsymbol{c}[k] - \boldsymbol{d}[k]\|^2 + \frac{||\boldsymbol{f}[k]||^2}{\text{SNR}} \tag{4.1}$$

where $\boldsymbol{c}[k]$ is the combined channel-equalizer response, $\boldsymbol{d}[k] = \boldsymbol{\delta}[k']$ is the desired channel-equalizer response ($k'$ denotes the index where $\boldsymbol{c}[k]$ has its maximum tap and $\boldsymbol{\delta}[k']$ denotes the all zeros vector except for a 1 in the $k'$-th position) and $\boldsymbol{f}[k]$ is the feedforward equalizer taps. The first part of the error corresponds the deviation of the

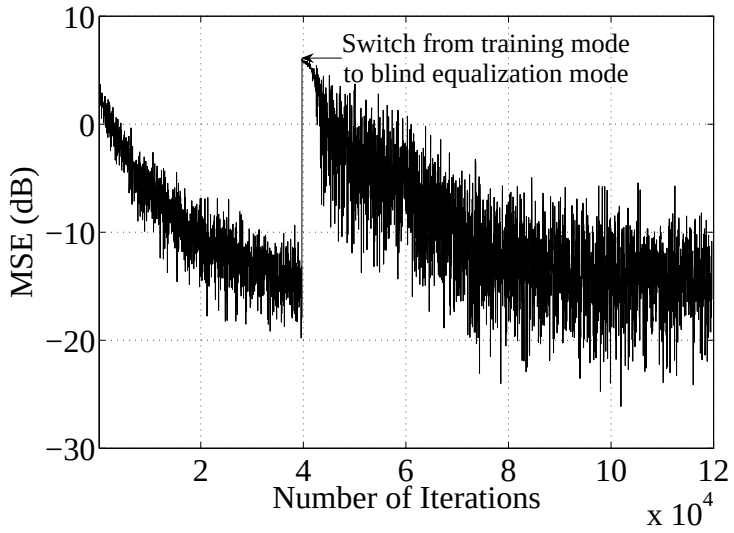


**Figure 4.4** MSE Trajectory of DFE for VDSL Channel

combined response from the desired one, and the second part corresponds the residual noise part. Figure 4.5 shows the reduction of the residual error (averaged over 10 trials) with time for the proposed model. These SISO system simulation results affirm that Bussgang-type blind equalization can be applied successfully Tomlinson-Harashima precoded systems.

## 4.2 ADDING A NEW USER TO A SISO SYSTEM

Often the communications channel changes over time for a VDSL environment or a new user wants to establish a connection with the transmitter through a different channel. The proposed system model of Fig. 3.2 has been derived for a fixed channel. We now investigate the performance of the proposed model for changing channel conditions.

In particular, we consider the case with a THP in the transmitter and an adaptive feedforward equalizer in the receiver. The THP parameters have been tuned for user 1's channel. We would then like to know if user 2, operating over a different channel, can blindly acquire and equalize the signal generated by user 1's transmitter.

Adding a new user's receiver to a SISO system turns it into a single-input multiple-output (SIMO) system. Figure 4.6 shows the SIMO system for a $1 \times N_R$ system, where $N_R$ represents the number of receivers. The THP filter tap weights are derived for the first channel; hence we denote that channel as the "basic channel." So, the performance

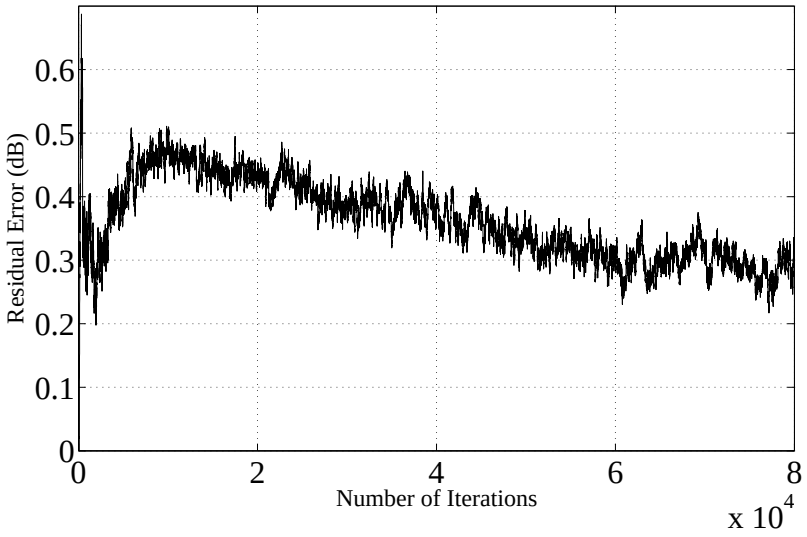


**Figure 4.5** Residual error for SISO system

of other users' blind equalizers needs investigation. The block diagram for adding a single new user to the proposed system is shown in Fig. 4.7.

It has already been mentioned that the THP tries to mitigate the i.s.i. introduced by the channel postcursors. Roughly, the purpose of the THP is to remove the distortions introduced by the zeros of the channel. Experimentally, we have found that, if all the new channels have the same zeros, then the additional equalizers will reliably start up. If, however, the zeros differ, the equalizers have greater difficulty.

We have determined that other factors affecting the equalizers' performance in this scenario include the pattern of the new channel compared to the basic channel and the length of the new channel. What we mean by the pattern of the channel is the gross characteristics and shape of the channel impulse response relative to the basic channel. If the two channels have similar patterns, the new equalizer works well. For example, if the basic channel is a bandpass channel, then its precoder will work well for another bandpass channel and it will not work as well for a null channel. The channel length is another important factor. If the new channel has a larger number of zeros than the basic channel, then THP cannot remove the effects of all of the zeros for the new channel. But this problem can be compensated using a longer feedforward equalizer in the new user's receiver.

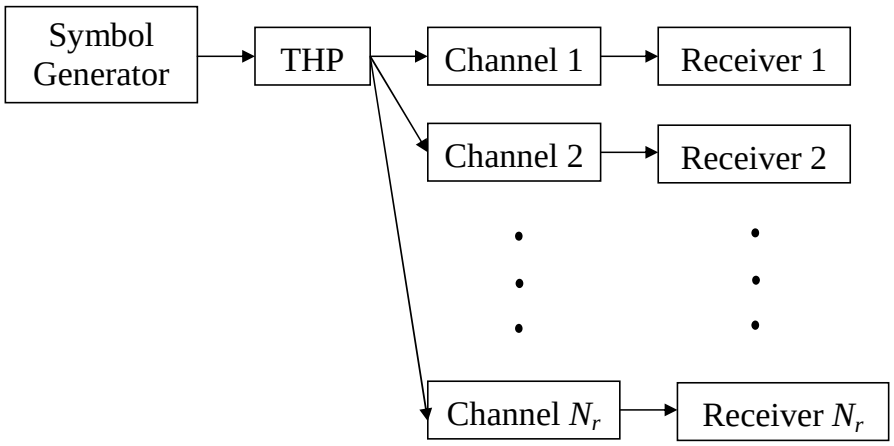


**Figure 4.6** Single-input multiple-output communications system

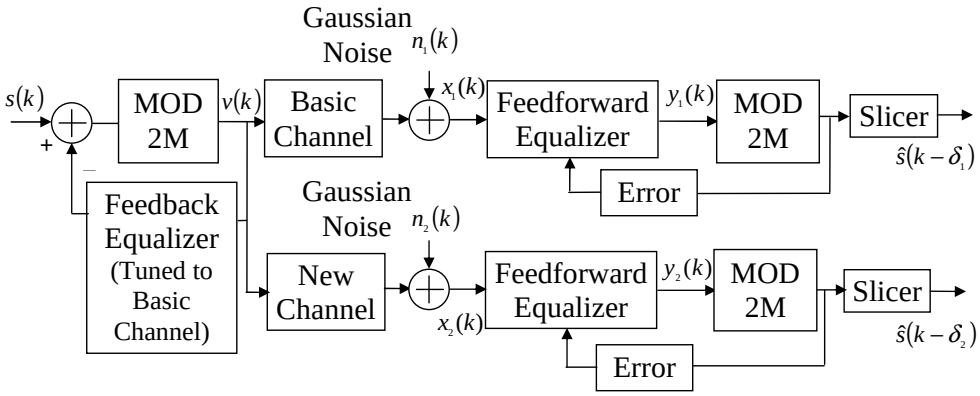


**Figure 4.7** Adding a new user to a SISO system

Adding a new user can be better understood with the aid of some Monte Carlo simulations. Let us consider the synthetic $T/2$-spaced bandpass channel $h$ = [0.1 -0.2 -0.1 1 -0.5 -0.1 -0.3 -0.1 0.1] taken from [50]. We use this channel as the basic channel. Using an 8-tap $T/2$- spaced feedforward equalizer and a 4-tap symbol-spaced feedback equalizer in training mode, we find the optimum THP tap weights. We then use these same THP tap weights while connecting to a new receiver through a new channel. Fig. 4.8 shows the magnitude frequency responses of the basic channel and the new user's $T/2$-spaced bandpass channel (created synthetically). As the pattern of the new channel is similar to the basic channel, the receiver, using the MMA algorithm, can

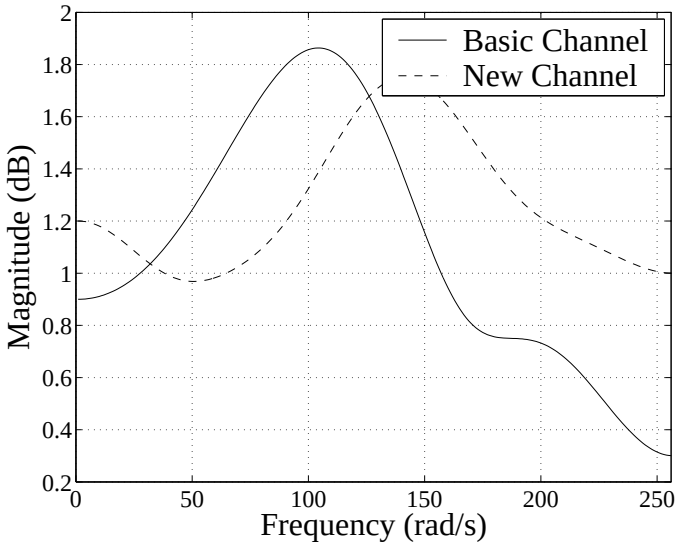


**Figure 4.8** Frequency responses of two different bandpass channels

easily initiate a connection to the first transmitter using the same number of feedforward equalizer taps. The residual error for this new receiver, averaged over 10 trials, is shown in Fig. 4.9. In addition, the 16-QAM constellation is successfully equalized as shown in Fig. 4.10.

Now, consider another channel for user 2 with a null around $0.42\pi$ rad/sec. Figure 4.11 shows its frequency response. This channel is significantly different from the basic channel. As it is a null channel, it has zeros almost on the unit circle. So, blind equalization techniques will tend to have difficulty. Hence, using an 8-tap $T/2$-spaced feedforward equalizer, the new equalizer is unable to connect successfully with the first transmitter. Two solutions are available for the null channel. We can either use a new DFE (adding an additional feedback filter for user 2) or increase the feedforward equalizer length as well as the simulation time.

As an example of the latter technique, using Monte Carlo simulations, it has been found that a 12-tap $T/2$-spaced feedforward equalizer can open the eye for the constellation as shown in Fig. 4.12. It might take more time for the reduction of the residual error as shown in Fig. 4.13, but the settling time can be reduced by increasing the length of the equalizer. This residual error curve has been averaged over 10 trials.

These simulations demonstrate the feasibility that a new receiver through a new channel can be added to an operating precoded SISO system with fixed THP tap

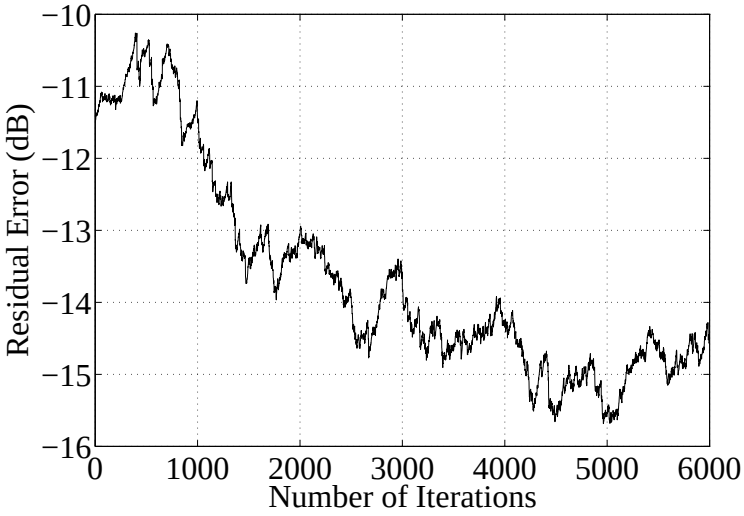


**Figure 4.9** Residual error for receiver of user 2

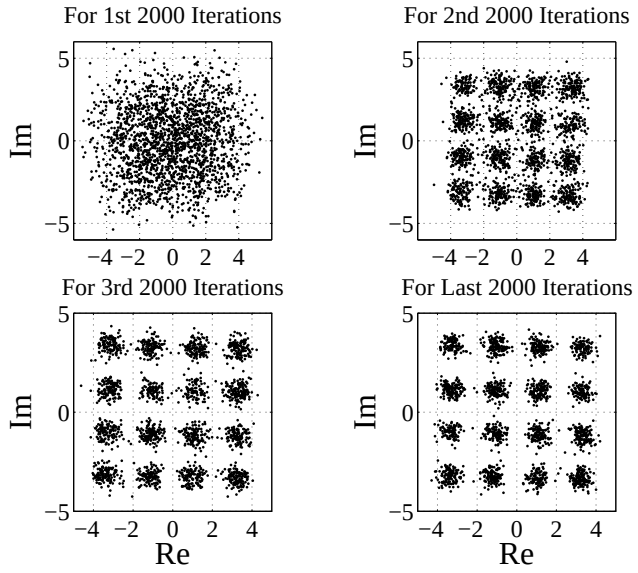


**Figure 4.10** Equalizer output for receiver of user 2

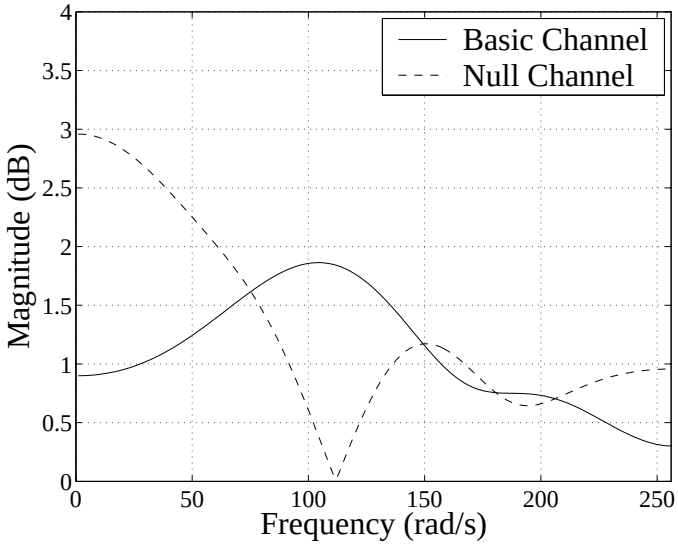


**Figure 4.11** Frequency response of null channel

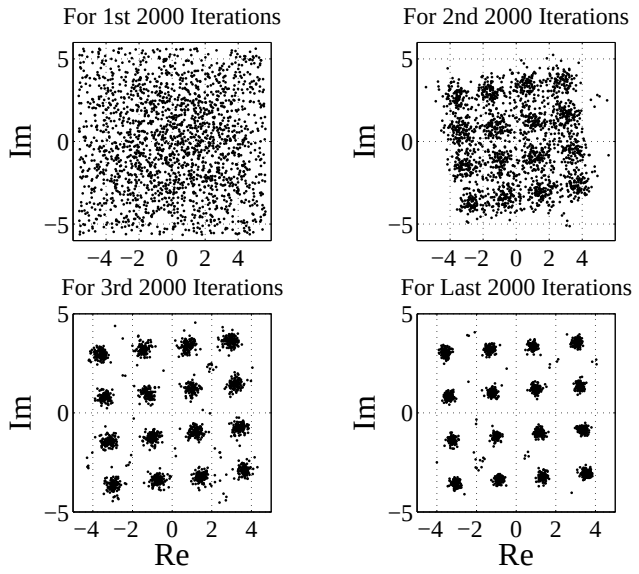


**Figure 4.12** Equalizer output of user 2's receiver for null channel

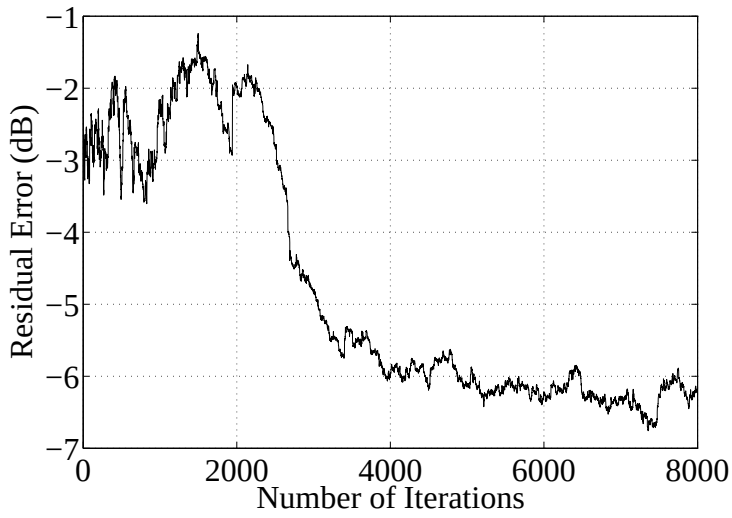


**Figure 4.13** Residual error of user 2's receiver for null channel

**Table 4.1** Channel Impulse Responses of 2 × 2 MIMO System from [3]

| $i$ | $k$ | $h_{1i}(k)$ | $h_{2i}(k)$ |
|---|---|---|---|
| 1 | 0 | $-0 - j0$ | $0 - j0$ |
| | 1 | $-0.17 - j1.03$ | $0.71 - j1.09$ |
| | 2 | $0.47 - j0.62$ | $-0.52 - j0.65$ |
| | 3 | $0 + j0$ | $-0 + j0$ |
| | 4 | $-0 + j0$ | $0 + j0$ |
| | 5 | $0 - j0$ | $-0 - j0$ |
| 2 | 0 | $0.0125 - j0.0681$ | $-0.0755 + j0.2306$ |
| | 1 | $-0.0590 + j0.5046$ | $0.4355 - j1.6674$ |
| | 2 | $0.0586 + j0.1737$ | $-0.1390 - j0.48$ |
| | 3 | $0.2915 + j0.1841$ | $-0.9865 - j0.2353$ |
| | 4 | $-0.0418 - j0.0185$ | $0.1448 + j0.0087$ |
| | 5 | $0.0144 + j0.0112$ | $-0.0479 - j0.0181$ |

weights. This application is one of the crucial findings of this thesis.

## 4.3 SIMULATIONS FOR MIMO SYSTEMS

In this section the proposed MIMO model outlined in Section 3.1 is considered for a 2 × 2 MIMO system. The channel impulse responses are taken from [3]. Table 4.1 shows the exact channel parameters. Two independent data streams of 4-QAM symbols pass through the 2 × 2 MIMO channel with additive white Gaussian noise at each receiver. The SNR is set to 30 dB. Similar to the SISO case, first we use an adaptive DFE to find the tap weights for the MIMO precoder. For this DFE, we use a 2 × 2 feedforward

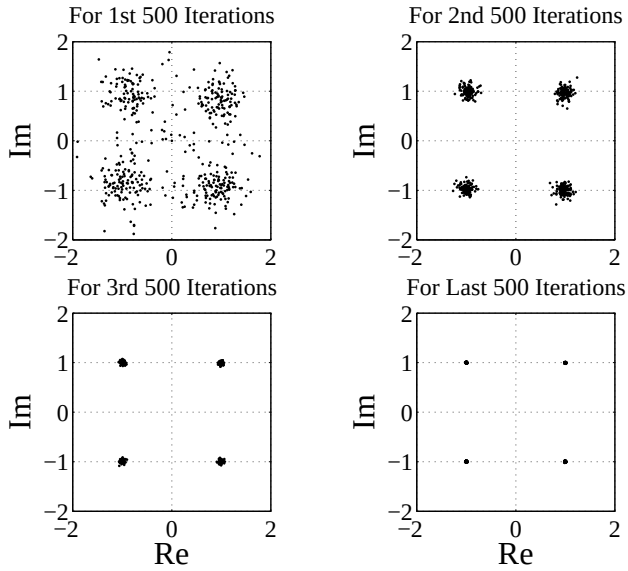


**Figure 4.14** Equalizer output constellations in training mode for first receiver

filter matrix and a $2 \times 2$ feedback filter matrix. The feedforward filters are each 8 taps long and the feedback filters are 6 taps long. All the filters are symbol-spaced. Training sequences containing the symbols from the two transmitters are fed into the inputs of the feedback filters. The LMS algorithm is used during this mode. The feedback and feedforward filter taps are initialized to zero, except for the last taps of the feedforward filters $\boldsymbol{f}_{11}$ and $\boldsymbol{f}_{22}$, which are each set to 1. The step size is 0.01 during the training mode. After sending 2000 symbols the DFE opens the "eye" for both the data streams successfully as shown in Figs. 4.14 and 4.15, respectively. The MSE trajectories during this training period are shown in Figs. 4.16 and 4.17. These curves are averaged over 10 trials. The training mode is stopped at this point, and the feedback filters' tap weights are transferred to the transmitter via a reverse channel to be used as the precoder tap weights.

This transfer yields the desired MIMO THP-equalizer system model. Now both receivers want to connect with the THP transmitters without using any training data. For a blind algorithm, we use the modified CMA algorithm [3] and use (2.43) to update the blind equalizer tap weights. The MIMO equalizer tap weights are initialized to zero, except for the center taps of $\boldsymbol{f}_{11}$ and $\boldsymbol{f}_{22}$, which are set to 1. The other parameters are $\mu = 0.001$ and $b_0 = 1.2$. Similar to the SISO case, we also need the modulo operator in

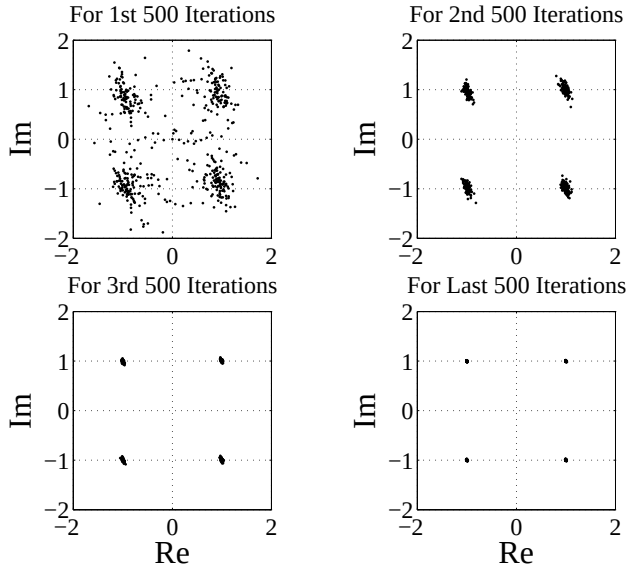


**Figure 4.15** Equalizer output constellations in training mode for second receiver

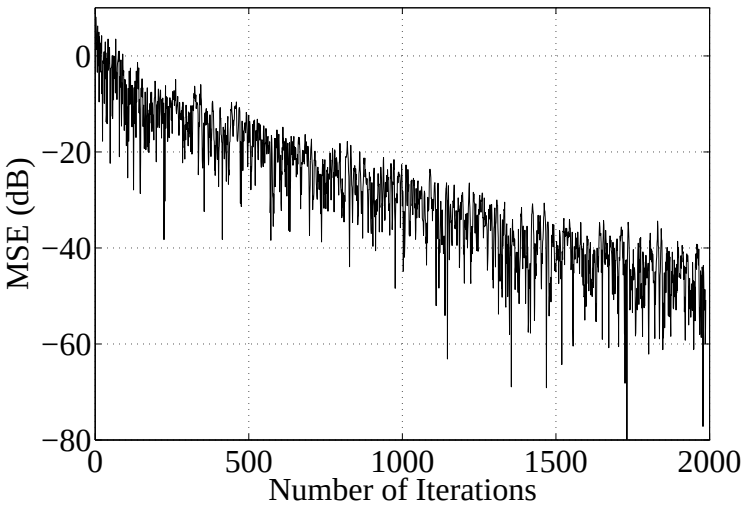


**Figure 4.16** MSE during training for first receiver

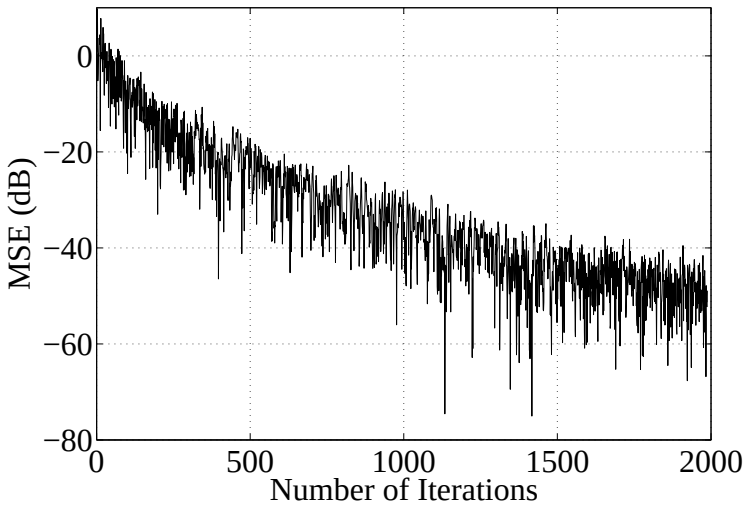


**Figure 4.17** MSE during training for second receiver

the receiver to invert the modulo addition of the THP transmitter. Figures 4.18 and 4.19 show the equalizer outputs for both receivers before the modulo addition. The modulo outputs of both receivers are presented in Figs. 4.20 and 4.21. The residual error of each of the receivers is calculated using the formula [3]

$$e_{\text{res}}^{j} = \frac{\sum_{i,k} |c_{ij}(k)|^2 - \max_{i,k} |c_{ij}(k)|^2}{\max_{i,k} |c_{ij}(k)|^2} \tag{4.2}$$

where $e_{\text{res}}^{j}$ is the residual error of the $j$-th receiver and $c_{ij}(k)$ is the combined channel-equalizer response. This error includes the intersymbol interference and interference from the other sources. Figures 4.22 and 4.23 show the evolution of this error (averaged over 10 trials) over time for both receivers. Note that the residual error curves for this MIMO system are more oscillating than the residual error for a SISO system (Fig. 4.5). In particular, the residual error curve of user 2 decreases and then increases and finally settles down with a higher level of error.

One reason for this behavior is that the CMA blind algorithm uses the higher-order moments of the received signal to detect the transmitted signal. It succeeds at mitigating the i.s.i. but has difficulty separating two signals with similar statistics. Thus, the kurtosis limiting effect of THP, which tends to make the transmitted signal statistics similar, can be detrimental in the MIMO scenario.

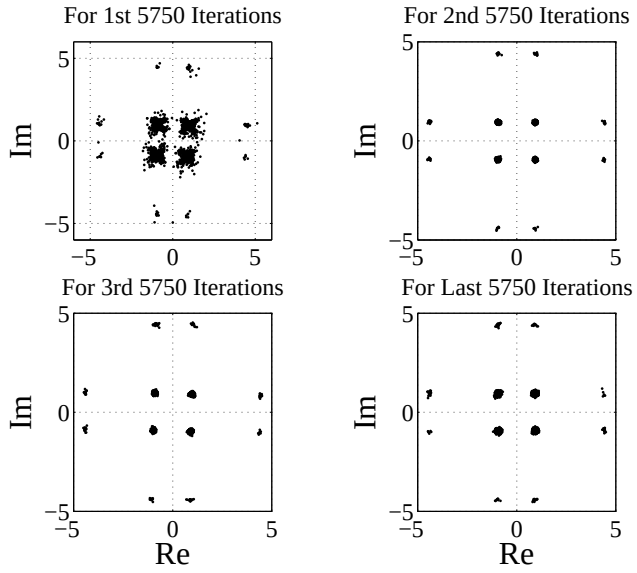


**Figure 4.18** Equalizer output constellations for first receiver

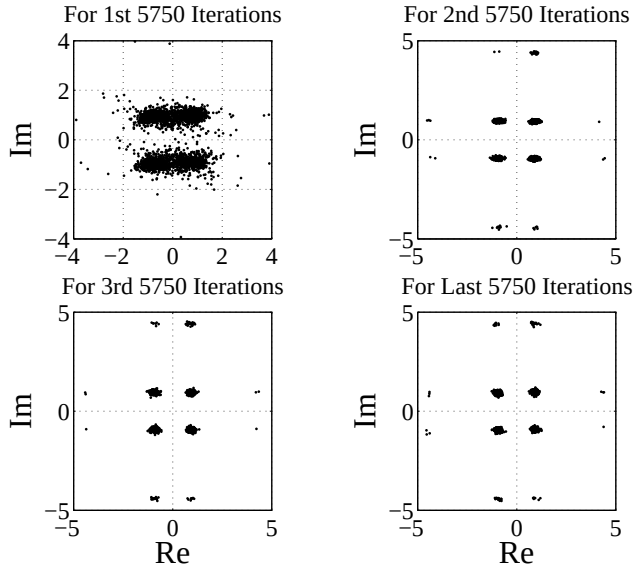


**Figure 4.19** Equalizer output constellations for second receiver

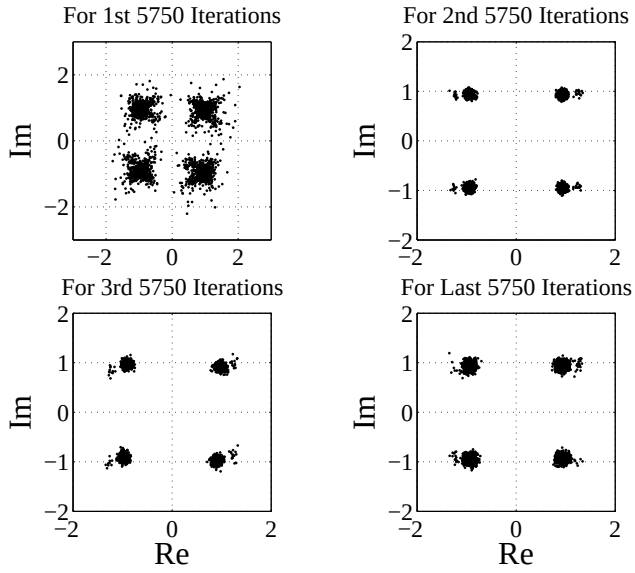


**Figure 4.20** Receiver modulo output constellations for first receiver

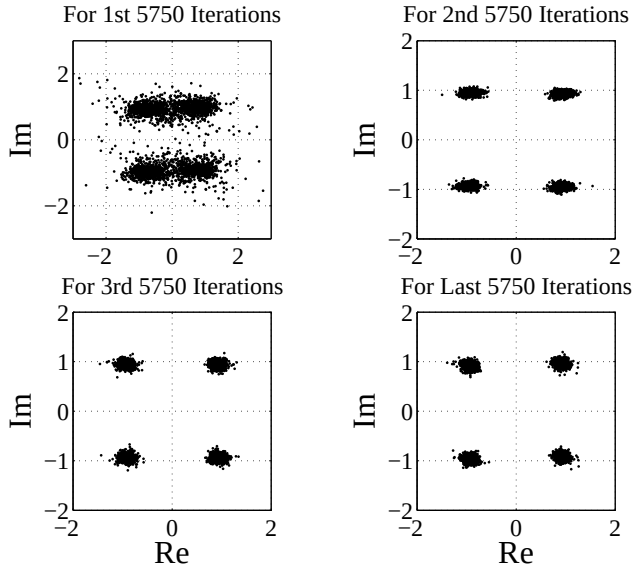


**Figure 4.21** Receiver modulo output constellations for second receiver

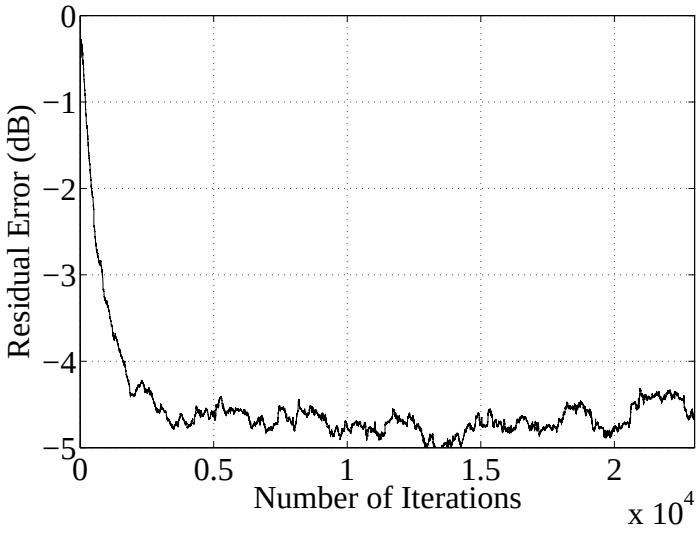


**Figure 4.22** Residual error for first receiver

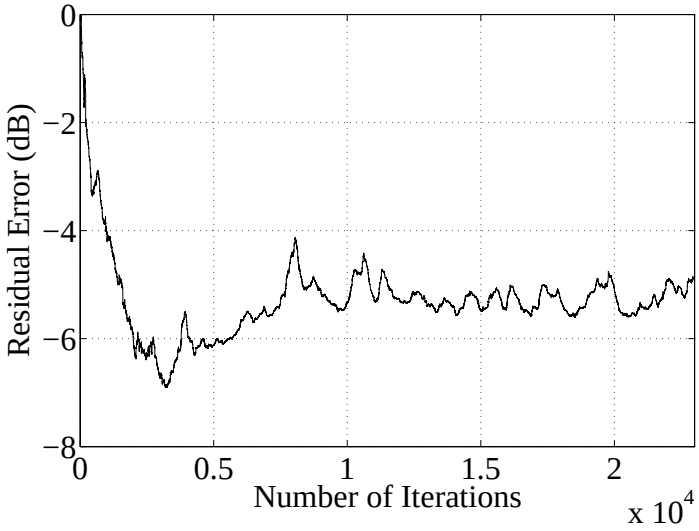


**Figure 4.23** Residual error for second receiver

# Chapter 5

# CONCLUSION

## 5.1 RESEARCH SUMMARY

Substantial bandwidth is necessary for high-speed communications. But, the full possible bandwidth efficiency is reduced in high speed wireline communications systems such as ADSL, VDSL, etc. A major source of bandwidth wastage is the training sequence overhead in these connections. A training sequence-less communication system is an excellent solution for increasing the bandwidth efficiency to enable broadband communications.

Blind equalization eliminates the requirement of training data. In Chapter 2 we have given a brief overview of Bussgang-type blind algorithms for equalization. Unfortunately, these computationally efficient algorithms have difficulty detecting Gaussian signals. Hence, a modification of the transmitted data is necessary to make the signal non-Gaussian.

A simple way of modifying the transmitted signal is by pre-equalization. But, linear pre-equalization increases the transmitted signal power. Hence, nonlinear pre-equalization techniques can be the solution. As we demonstrate in this thesis, not only can THP be used to reduce the transmitted signal power and the error propagation problem of DFEs, THP can also be used to ensure that the transmitted signal statistics are non-Gaussian. In support of these results, in Chapter 2 we have introduced the DFE and THP for both SISO and MIMO communications systems.

To study blind equalization of a THP-encoded signal, in Chapter 3 we use the following system. A DFE is trained using the LMS algorithm. Then, the feedback filter tap weights are sent back to the transmitter to be used in the THP filter. Finally,

the linear feedforward portion of the DFE is retrained using a Bussgang-type blind algorithm.

The crucial parameter for Bussgang-type bind algorithms is the kurtosis of the transmitted signal. In Chapter 3 we have derived analytical bounds on the kurtosis for THP-encoded signals for both SISO and MIMO systems. We show that the modulo operation in the THP ensures that the THP-encoded signal has sub-Gaussian statistics. The kurtosis bounds are found to be the same for both SISO and MIMO systems.

In Chapter 4 we verify our analysis using Monte Carlo simulations. We first consider a SISO system with a 4-QAM data source through a near baseband VDSL Channel. We derive the feedback taps using a training sequence mode. Using those taps for the THP prefilter makes the work of the blind equalizer at the receiver side much easier. We also experimentally show that a new user through a new channel can be blindly added to an existing SISO THP-blind system given certain channel conditions. Finally, we simulate a $2 \times 2$ MIMO system with a 4-QAM data source. We show that multiple receivers can blindly acquire the MIMO THP generated signals.

In summary, we have found that the kurtosis of a THP-encoded signal remains sub-Gaussian for any data symbol statistics. In fact, for a $M$-ary QAM data source, with $M$ even, the kurtosis of the precoded data converges to the kurtosis of a uniform distribution. This convergence is shown both analytically and using simulations. As a result, blind equalizers can work for a wide variety of source distributions, given THP encoding.

## 5.2 FURTHER RESEARCH

During the course of this thesis research, a number of issues were raised that were beyond the scope of the thesis or could not be completed in a reasonable amount of time. Many of these issues are related to MIMO systems. For example, the scenario of adding a new user to an operating MIMO system needs to be considered. Also, blind equalizations algorithms need to be found which are more robust to a wide variety of channel conditions and which converge rapidly. For MIMO systems, only 4-QAM data sources were simulated. Our preliminary investigation indicates that MIMO blind

algorithms have difficulty opening the eye for higher-order constellations due to very similar signal statistics. This needs to be explored further. Another possible research topic is to compare the feedback equalizer tap weights for MIMO systems derived from training data to the optimum tap weights. Wiener filter theory for the MIMO DFE can be used for this comparison. Finally, it would be useful to study the performance of the proposed MIMO model for more than two transmitters and receivers.

## REFERENCES


[1] L. M. Garth, "A dynamic convergence analysis of blind equalization algorithms," *IEEE Trans. Commun.*, vol. 49, no. 4, pp. 624–634, Apr. 2001.

[2] G. Picchi and G. Prati, "Blind equalization and carrier recovery using a "stop-and-go" decision-directed algorithm," *IEEE Trans. Commun.*, vol. 35, no. 9, pp. 877–887, Sept. 1987.

[3] Y. G. Li and K. J. R. Liu, "Adaptive blind source separation and equalization for multiple-input/multiple-output systems," *IEEE Trans. Inform. Theory*, vol. 44, no. 7, pp. 2864–2876, Nov. 1998.

[4] T. Starr, J. M. Cioffi, and P. Silverman, *Understanding Digital Subscriber Line Technology.* Upper Saddle River, NJ: Prentice-Hall, 1999.

[5] G. J. Foschini, "Equalization without altering or detect data," *AT&T Tech. J.*, vol. 64, no. 8, pp. 1885–1911, Oct. 1985.

[6] G. Ginis and J. M. Cioffi, "A multi-user precoding scheme achieving crosstalk cancellation with application to DSL systems," in *Proc. Thirty-Fourth Asilomar Conf. on Signals, Systems and Computers*, vol. 2, Pacific Grove, CA, Oct. 29 - Nov. 1, 2000, pp. 1627–1631.

[7] S. Haykin, *Adaptive Filter Theory*, 4th ed. Englewood Cliffs, NJ: Prentice-Hall, 2002.

[8] Z. Ding and Y. G. Li, *Blind Equalization and Identification.* New York: Marcel Dekker, Inc., 2001.

[9] J. P. LeBlanc, K. Dogancay, R. A. Kennedy, and C. R. Johnson, Jr., "Effects of input data correlation on the convergence of blind adaptive equalizers," in *Proc. IEEE Int'l. Conf. on Acoustics, Speech, and Signal Processing*, Adelaide, Australia, Apr. 19-22, 1994, pp. III–313–316.

[10] J. P. LeBlanc, I. Fijalkow, B. Huber, and C. R. Johnson, Jr., "Fractionally spaced CMA equalizers under periodic and correlated inputs," in *Proc. IEEE Int'l. Conf. on Acoustics, Speech, and Signal Processing*, Detroit, Michigan, May 9-12, 1995, pp. 1041–1044.

[11] J. P. LeBlanc, I. Fijalkow, and C. R. Johnson, Jr., "Fractionally-spaced constant modulus algorithm blind equalizer error surface characterization: Effects of source distributions," in *Proc. IEEE Int'l. Conf. on Acoustics, Speech, and Signal Processing*, Atlanta, Georgia, May 7-10, 1996, pp. 2944–2947.

[12] C. R. Johnson, P. Schinter, T. J. Endres, J. D. Behm, D. R. Brown, and R. A. Casas, "Blind equalization using the constant modulus criterion: A review," *Proc. IEEE*, vol. 86, no. 10, pp. 1927–1950, Oct. 1998.

[13] Y. Li and Z. Ding, "Convergence analysis of finite length blind adaptive equalizers," *IEEE Trans. Signal Processing*, vol. 43, no. 9, pp. 2120–2129, Sept. 1995.

[14] ——, "Global convergence of fractionally spaced Godard equalizer," *IEEE Trans. Signal Processing*, vol. 44, no. 4, pp. 818–826, Apr. 1996.

[15] M. Tomlinson, "New automatic equalizer employing modulo arithmetic," *Electron. Lett.*, vol. 7, pp. 138–139, Mar. 1971.

[16] H. Harashima and H. Miyakawa, "Matched-transmission technique for channels with inter-symbol interference," *IEEE Trans. Commun.*, vol. 20, no. 4, pp. 774–780, Aug. 1972.

[17] R. F. H. Fischer, W. H. Gerstacker, and J. B. Huber, "Dynamics limited precoding, shaping, and blind equalization for fast digital transmission over twisted pair lines," *IEEE J. Select. Areas Commun.*, vol. 13, no. 9, pp. 1622–1633, Dec. 1995.

[18] M. R. Gibbard and A. B. Sesay, "Asymmetric signal processing for indoor wireless LAN's," *IEEE Trans. Veh. Technol.*, vol. 48, no. 6, pp. 2053–2064, Nov. 1999.

[19] R. W. Lucky, "Automatic equalization for digital communication," *Bell Syst. Tech. J.*, vol. 44, no. 4, pp. 547–588, Apr. 1965.

[20] A. Gersho, "Adaptive equalization of highly dispersive channels for data transmission," *Bell Syst. Tech. J.*, vol. 48, no. 1, pp. 55–70, Jan. 1969.

[21] J. G. Proakis and J. H. Miller, "An adaptive receiver for digital signaling through channels with intersymbol interference," *IEEE Trans. Inform. Theory*, vol. 15, no. 4, pp. 484–497, July 1969.

[22] B. Widrow and M. E. Hoff, "Adaptive switching circuits," in *IRE WESCON Conv. Rec.*, vol. 4, New York, Aug. 1960, pp. 96–104.

[23] S. U. H. Qureshi, "Adaptive equalization," *Proc. IEEE*, vol. 73, pp. 1349–1387, Sept. 1985.

[24] Y. Sato, "A method of self-recovering equalization for multilevel amplitude-modulation systems," *IEEE Trans. Commun.*, vol. 23, pp. 679–682, June 1975.

[25] D. N. Godard, "Self-recovering equalization and carrier tracking in two-dimensional data communication systems," *IEEE Trans. Commun.*, vol. 28, pp. 1867–1875, Nov. 1980.

[26] J. R. Treichler and B. G. Agee, "A new approach to multipath correction of constant modulus signals," *IEEE Trans. Acoust., Speech, Signal Processing*, vol. 31, pp. 459–472, Apr. 1983.

[27] J. R. Treichler, M. G. Larimore, and J. C. Harp, "New processing techniques based on the constant modulous adaptive algorithm," *IEEE Trans. Acoust., Speech, Signal Processing*, vol. 33, pp. 420–431, Apr. 1985.

[28] A. Benveniste and M. Goursat, "Blind equalizers," *IEEE Trans. Commun.*, vol. 32, pp. 871–882, Aug. 1984.

[29] K. N. Oh and Y. Y. Chin, "Modified constant modulus algorithm: blind equalization and carrier phase recovery algorithm," in *Proc. IEEE Int'l. Conf. Communications*, vol. 1, Seattle, WA, Jun. 18-22, 1995, pp. 498–502.

[30] O. Shalvi and E. Weinstein, "New criteria for blind deconvolution of nonminimum phase systems (channels)," *IEEE Trans. Inform. Theory*, vol. 36, no. 2, pp. 312–321, Mar. 1990.

[31] S. A. Athuraliya and L. M. Garth, "Quantized CMA equalization for shaped signal constellations," *IEEE Signal Processing Lett.*, vol. 11, no. 2, pp. 67–70, Feb. 2004.

[32] V. Weerackody, S. A. Kassam, and K. R. Laker, "A simple hard-limited adaptive algorithm for blind equalization," *IEEE Trans. Circuits Syst. II*, vol. 39, no. 7, pp. 482–487, July 1992.

[33] L. He and M. Amin, "A dual-mode technique for improved blind equalization for QAM signals," *IEEE Signal Processing Lett.*, vol. 10, no. 2, pp. 29–31, Feb. 2003.

[34] M. Austin, "Decision-feedback equalization for digital communication over dispersive channels," *MIT Research Laboratory of Electronics Technical Report 461*, Aug. 1967.

[35] P. Monsen, "Feedback equalization for fading dispersive channels," *IEEE Trans. Commun.*, vol. 17, no. 1, pp. 56–64, Jan. 1971.

[36] C. A. Belfiore and J. H. Park, Jr., "Decision feedback equalization," *Proc. IEEE*, vol. 67, no. 8, pp. 1143–1156, Aug. 1979.

[37] R. Laroia, S. A. Tretter, and N. Farvadin, "A simple and effective precoding scheme for noise whitening on intersymbol interference channels," *IEEE Trans. Commun.*, vol. 41, no. 10, pp. 1460–1463, Oct. 1993.

[38] R. Laroia, "Coding for intersymbol interference channels - combined coding and precoding," *IEEE Trans. Inform. Theory*, vol. 42, no. 4, pp. 1053–1061, July 1996.

[39] C. B. Papadias and A. J. Paulraj, "A constant modulus algorithm for multiuser signal separation in presence of delay spread using antenna arrays," *IEEE Signal Processing Lett.*, vol. 4, no. 6, pp. 178–181, June 1997.

[40] C. B. Papadias, "Globally convergent blind source separation based on a multiuser kurtosis maximization criterion," *IEEE Signal Processing Lett.*, vol. 48, no. 12, pp. 3508–3518, Dec. 2000.

[41] ——, "Unsupervised receiver processing techniques for linear space-time equalization of wideband multiple input/multiple output channels," *IEEE Trans. Signal Processing*, vol. 52, no. 2, pp. 472–482, Feb. 2004.

[42] R. F. H. Fischer, C. Stierstorfer, and J. B. Huber, "Precoding for point-to-multipoint transmission over MIMO ISI channels," in *Proc. Int'l. Zurich Seminar (IZS '04) on Communications*, Zurich, Switzerland, Feb. 18-20, 2004, pp. 208–211.

[43] J. Brehmer, G. Dietl, M. Joham, and W. Utschick, "Reduced-compexity linear and nonlinear precoding for frequency-selective MIMO channels," in *Proc. IEEE Int'l. Conf. on Vehicular Technology*, vol. 5, Los Angeles, CA, Sep. 26-29, 2004, pp. 3684–3688.

[44] V. Stankovic and M. Haardt, "Successive optimization Tomlinson-Harashima precoding (SO THP) for multi-user MIMO systems," in *Proc. IEEE Int'l. Conf. on Acoustics, Speech, and Signal Processing*, vol. 3, Mar. 18-23, 2005, pp. 1117–1120.

[45] R. F. H. Fischer, *Precoding and Signal Shaping for Digital Transmission*. New York: John Wiley & Sons, Inc., 2002.

[46] N. Al-Dhahir and A. H. Sayed, "The finite-length multi-input multi-output MMSE-DFE," *IEEE Trans. Signal Processing*, vol. 48, no. 10, pp. 2921–2936, Oct. 2000.

[47] Y. Li and K. J. R. Liu, "Blind identification and equalization for multiple-input/multiple-output channels," in *Proc. IEEE Int'l. Conf. on Global Telecommunications*, vol. 3, London, Nov. 18-22, 1996, pp. 1789–1793.

[48] J. E. Mazo and J. Salz, "On the transmitted power in generalized partial response," *IEEE Trans. Commun.*, vol. 24, no. 3, pp. 348–352, Mar. 1976.

[49] M. V. Eyuboglu and G. D. Forney, Jr., "Trellis precoding: Combined coding, precoding and shaping for intersymbol interference channels," *IEEE Trans. Inform. Theory*, vol. 38, no. 2, pp. 301–314, Mar. 1992.

[50] Cornell University Broadband Adaptive Receiver Design (BARD) Research Group Website, "http://bard.ece.cornell.edu/downloads/tutorials/fsedemo/fsedemo.m."